12-15-2014

# Molecular Mechanisms of Gap Junction Regulation by the E3 Ubiquitin Ligase WWP1

Measho Hagos Abreha
*University of South Carolina - Columbia*

# Molecular Mechanisms of Gap Junction Regulation by the E3 Ubiquitin Ligase WWP1

By

Measho Hagos Abreha

Bachelor of Science
Addis Abeba University, 1997

Master of Science
Addis Abeba University, 2001

---

Submitted in Partial Fulfilment of the Requirements

For the Degree of Doctor of Philosophy in

Biological Sciences

College of Arts and Sciences

University of South Carolina

2014

Accepted by

Lydia E. Matesic, Major Professor

Rekha Patel, Committee Member

Lewis H. Bowman, Committee Member

Johannes Stratmann, Committee Member

Edie C. Goldsmith, Committee Member

Lacy Ford, Vice Provost and Dean of Graduate Studies

## DEDICATION

This work is dedicated to my beloved son Kaleb Hagos Tesfaye who has brought joy, hope and meaning to my life. He has been a source of motivation and kept me going through tough times. I would not have been able to accomplish this work without his love and presence in my life.

## ACKNOWLEDGEMENTS

I first and foremost would like to acknowledge my advisor Dr. Lydia E. Matesic for her continues guidance, encouragement and support throughout my Ph.D. training. Her exceptional academic expertise and critical thinking has motivated me greatly and helped me grow as a scientist. I thank my advisor not only for her academic expertise but also for her being understanding and supportive of my personal life. I am sincerely grateful for making my stay in graduate school while raising a child less stressful. Additionally, I would like to thank my lab mates, Dr. Wassim Basheer, Heather Mentrup, Elizabeth Thames and Eric Goff for their support, critical comments and making my stay in the lab enjoyable. I would like also to thank my friends and family for their support and encouragement throughout my training. I would like to thank Tesfaye Kidane and Kaleb Tesfaye for their support and encouragement. I especially would like to thank my dad Hagos Abreha and my late mother Tirunesh Dejene for their love, support and encouragement and for going far and beyond so I could succeed in my education. I would also like to thank my sister Mulualem Hagos for her extraordinary love, care, and encouragement throughout my life. I would like to thank Dr. Yohannes Negash for reading and editing my dissertation as well as his continued encouragement and support. Finally, I would like to thank members of my dissertation committee Dr. Rekha Patel, Dr. Lewis Bowman, Dr. Eddie Goldsmith, and Dr. Johannes Stratmann for their guidance, critical comments and valuable input throughout my Ph.D. training.

## ABSTRACT

Ubiquitylation is a post-translational modification that influences a wide variety of cellular processes including protein degradation, protein subcellular localization, cell cycle progression, transcription, and DNA damage repair. Covalent attachment of the small ubiquitin molecule to a target protein involves the sequential action of three enzymes (E1, E2, and E3). In this process, substrate specificity is conferred by the E3 ligase. Our work has focused on the function of one such E3 ubiquitin ligase, WWP1. Known targets of WWP1 include cell cycle proteins, tumor suppressors, and transcription factors that promote differentiation of mesenchymal stem cells to the osteoid lineage. Recently, we have identified a novel target of WWP1 – the gap junction protein connexin (CX) 43. In particular, we found that mice overexpressing WWP1 had a 90% reduction in CX43 within the myocardium and died from ventricular arrhythmias as a consequence.

CX43 is a transmembrane protein that oligomerizes to form intercellular channels which facilitate communication between adjacent cells via the transfer of small molecules. This metabolic and electrical coupling of adjacent cells plays a vital role in almost all cellular processes including growth and differentiation, cell division, and homeostasis as well as in electroconduction of the heart. Therefore, it is not surprising that CX43 is broadly expressed in nearly every cell type, and it is likely that there are commonalities underlying the regulation of CX43 in all cells that express it. Of particular interest is the fact that CX43 has a remarkably short half-life for an integral membrane protein (on the order of 1-5 hours) in all cell types examined.

To investigate the molecular mechanisms involved in CX43 turnover, we used an established tissue culture system to examine the effects of changes in expression of WWP1 on the stability and subcellular localization of CX43. We found that CX43 could co-immunoprecipitate with WWP1, and this interaction was dependent on the PPXY motif of CX43. This association promoted the K27- and K29-linked polyubiquitylation of CX43 by WWP1. Co-immunoprecipitation of WWP1 with CX43 and subsequent ubiquitylation of CX43 was enhanced in the presence of phorbol 12-myristate 13-acetate (PMA) which has been reported to induce mitogen activated protein kinase (MAPK)-dependent phosphorylation and subsequent internalization of CX43 from the cell membrane to the early endosomes. WWP1-mediated ubiquitylation was found to destabilize CX43, as the overexpression of wild type WWP1 in HeLa-CX43 cells reduced the half-life of CX43 from 2 hours to less than 1 hour, while a mutant version of WWP1 lacking ubiquitin ligase activity (C866S) had no significant effect on the stability of CX43. The increased turnover of CX43 associated with the overexpression of WWP1 also significantly reduced gap junction-mediated intercellular communication. Further investigation of the role of WWP1-mediated ubiquitylation on CX43 trafficking revealed that the ligase activity of WWP1 promoted trafficking of WWP1 from the early endosome to the late endosome with subsequent delivery to the lysosome for degradation.

These observations were corroborated when endogenous WWP1 was knocked down using a siRNA pool that targets *WWP1*. Specifically, loss of WWP1 was associated with increased levels of CX43 on the plasma membrane and with decreased trafficking of CX43 from the early endosome to the late endosome. Instead, with WWP1 knockdown, increased co-localization of CX43 with the recycling endosome marker RAB11 was

noted. These data, in conjunction with our overexpression studies, suggest that WWP1 ubiquitylates CX43 in the early endosome, and this signal is required for trafficking to the lysosome for degradation. In the absence of functional WWP1, CX43 is trafficked back to the plasma membrane via an endogenous recycling pathway whose existence hitherto has been sparsely described in the literature.

Collectively, this study has identified a novel role for WWP1-mediated ubiquitylation in the trafficking and lysosomal degradation of CX43 involving an atypical ubiquitin linkage. Gap junction dysregulation is associated numerous pathological conditions including arrhythmia, skin defects, cataracts and carcinogenesis. Therefore, studies like this one that elucidate the molecular mechanisms underlying the regulation of CX43 will greatly contribute towards the development of novel therapeutics.

## TABLE OF CONTENTS

## LIST OF FIGURES

## LIST OF ABBREVIATIONS

C886S..... Ligase dead version of WWP1

CHX..... Cyclohexamide

CK1..... Casein kinase 1

CME.....Clathrin Mediated Endocytosis

CX.....Connexin

E1.....Ubiquitin activating enzyme

E2.....Ubiquitin conjugating enzyme

E3.....Ubiquitin ligase

EGF..... Epidermal Growth Factor

EGRF.....Epidermal Growth Factor Receptor

EPS15.....Epithelial Growth Factor Receptor 15

ESCRT.....Endosomal Sorting Complexes Required for Transport

GJ.....Gap junction

GJIC.....Gap junction intercellular communication

HECT.....Homologues to the E6-AP Carboxyl Terminus

HRS..... Hepatocyte Growth Factor Regulated Tyrosine Kinase Substrate

ILV..... Intraluminal Vesicles

MAPK.....Mitogen Activated Protein Kinase

MVB.....Multivesicular Bodies

NEDD4.....Neural Precursor Cells Expressed Developmentally Down Regulated

PMA ..... Phorbol 12-myristate 13-acetate

RING ..... Really Interesting New Gene

SMURF ..... Smad Ubiquitin Regulatory Factor

TBST ..... Tris-Buffered Saline with Tween 20

UIM ..... Ubiquitin Interacting Motif

# CHAPTER ONE

## GENERAL INTRODUCTION

Ubiquitylation is a post-translational modification that influences protein stability, protein activity, protein-protein interactions and subcellular localization and, consequently, plays a critical role in the regulation of many cellular processes such as cell signaling, transcription, translation, DNA repair and cellular homeostasis (Heride et al., 2014; Metzger et al., 2012; Weissman, 2001). The term ubiquitylation (or ubiquitination) refers to the covalent addition of ubiquitin to proteins. Ubiquitin is a small, highly conserved 76 amino acid long polypeptide expressed in all eukaryotic cells (Fang and Weissman, 2004). The ubiquitin moiety is primarily conjugated to the $NH_2$ group of lysine residues in target proteins or, rarely, ubiquitin can be attached to the $NH_2$ group of the first amino acid in a protein (Bonifacino and Weissman, 1998; Lorick et al., 2006). Ubiquitin is attached to substrates through an isopeptide bond between the carboxyl-terminal glycine of ubiquitin and the ε-amino group of a lysine residue in substrates (Trempe, 2011; Weissman, 2001). The process of ubiquitylation involves the sequential action of three enzymes (E1, E2 and E3). The ubiquitin activating enzyme (E1) forms a thiol-ester bond between a highly conserved cysteine residue in its active site and the COOH group of glycine 76 of ubiquitin. This reaction requires ATP and results in the activation of ubiquitin. The activated ubiquitin is then transferred to the active site cysteine residue of the ubiquitin conjugating enzyme (E2) though a transesterification reaction (Clague and Urbe, 2010; Weissman, 2001). The activated ubiquitin is then either conjugated to the substrate by the E2 or transferred to an ubiquitin ligase (E3) depending on the type of E3 involved in the reaction. The HECT (Homologues to E6-AP Carboxyl-Terminus) family of E3 ligases have a cysteine residue at the active site capable of making a high energy thioester bond with the activated ubiquitin to directly conjugate the

ubiquitin to the substrate. The RING (Really Interesting New Gene) and RING-related E3 ligases (van Wijk and Timmers, 2010) have no catalytic activity and bind both the Ub-loaded E2s and the substrate at the same time and act like scaffolds to bring the E2 and the substrate in close proximity (Metzger et al., 2012)(Fig. 1.1). To date, more than 600 E3 ubiquitin ligases, 40 E2s and three E1 enzymes have been identified in mammals (Metzger et al., 2012). Of the more than 600 E3 ligases encoded by the mammalian genome, the majority belong to the RING and RING related family of E3 ligases with only about 30 HECT E3 ligases identified so far (Metzger et al., 2012).

In the ubiquitylation process, substrates are conjugated with a single ubiquitin (mono-ubiquitylation), multiple ubiquitin molecules to multiple different lysine residues (multi-mono-ubiquitylation) or a polyubiquitin chain. Polyubiquitylation occurs by the conjugation of ubiquitin to one of the seven internal lysine residues within ubiquitin (K6, K11, K27, K29, K33, K48, and K63). Polyubiquitin chains with these varying linkages adopt distinct conformations that are differentially recognized by ubiquitin interacting motif (UIM) containing proteins which function in 26S proteasomal degradation, membrane protein endocytosis, and intracellular trafficking (Andersen et al., 2005; Di Fiore et al., 2003) (Hurley et al., 2006); (Hicke and Dunn, 2003; Hurley et al., 2006).

The fate of ubiquitylated proteins depends on the length and type of linkage in a polyubiquitin chain. Generally, mono-ubiquitylation or multi-mono-ubiquitylation is associated with internalization of membrane proteins (Clague and Urbe, 2010). K48-linked polyubiquitin chains are associated with degradation by the 26S proteasome whereas K63-linked polyubiquitin chains are implicated in endocytosis, post endocytic trafficking of proteins leading to lysosomal degradation as well as in non-degradative

outcomes of ubiquitylation such as change in subcellular localization, signaling and activation of protein function (Trempe, 2011) (Fig.1.2). The role of atypical polyubiquitin chains (i.e., K6, K11, K27, K29 and K33 linkages) is less well characterized although the function of these linkages is starting to come to light. For instance, K11-linked polyubiquitin chains have been implicated in cell signaling events as well as promoting changes in subcellular localization (Bremm et al., 2010), whereas K29-linked polyubiquitin chains have been associated with enhanced trafficking of target towards the lysosome for degradation (Chastagner et al., 2006).

**The HECT E3 ubiquitin ligase WWP1**

Because E3 ubiquitin ligases dictate substrate specificity in the ubiquitylation process, it is not surprising that they play key regulatory roles in a myriad of cellular processes such as membrane trafficking, transcription, translation, DNA repair and homeostasis (Bernassola et al., 2008; Chen and Matesic, 2007; Zhi and Chen, 2011). Our work is focused on one such E3 ubiquitin ligase, WWP1. In mammals, WWP1 is one of nine members of the NEDD4 family of E3 ligases (Table 1). Dysregulation in the functions of many members of this family has been associated with many pathologies including cancer, osteoporosis, viral infections, as well as neurodegenerative and cardiac diseases (Chen and Matesic, 2007; Zhi and Chen, 2012).

All members of the NEDD4 family of E3 ligases share three functional domains: a C2 domain on the $NH_2$ terminus, between two to four tandem WW domains, and a carboxyl-terminal catalytic HECT domain The C2 domain is a phospholipid binding domain which is required for membrane localization (Macias et al., 2002; Plant et al., 1997). Based on studies conducted with the C2 domains derived from the NEDD4 and

SMURF1 E3 ligases, (Ogunjimi et al., 2005; Plant et al., 1997) it is hypothesized that the membrane associative function of the C2 domain of these proteins is responsive to changes in intracellular $Ca^{2+}$ (Wiesner et al., 2007). The WW domains are approximately 40 amino acid long motifs that mediate protein-protein interaction through recognition of proline-rich sequences such as PPXY, PPLP, PPR, and phosphorylated serine/threonine-proline motifs (Chen and Matesic, 2007; Salah et al., 2012; Staub et al., 1996). The domain name originates from the presence of two highly conserved tryptophan (W) residues spaced between 20 and 22 amino acids apart (Macias et al., 2002; Salah et al., 2012). Finally, the HECT domain made of about 350 amino acids has a conserved cysteine residue involved in the transfer of activated ubiquitin to substrates (Kee and Huibregtse, 2007) (Fig.1.3).

The human *WWP1* gene maps to chromosome 8q21 and codes for a 920 amino acid long protein with a molecular weight of ~110 kDa (Chen and Matesic, 2007; Ingham et al., 2004; Zhi and Chen, 2011). WWP1 targets a wide range of proteins that are involved in multiple cellular processes including protein trafficking, apoptotic signaling, transcription, DNA damage repair, and viral budding (Chen and Matesic, 2007; Zhi and Chen, 2011). The list of previously identified targets of WWP1 include: SMAD2, KLF5, p63, p53, ERBB4/HER4, RUNX2, JUNB, RNF11, SPG20, TBR1, SMAD4, KLF4, EPS15 and GAG (Chen and Matesic, 2007; Chen et al., 2008; Komuro et al., 2004; Moren et al., 2005; Zhi and Chen, 2012) (Table 2). WWP1 has been shown to negatively regulate the TGF-β tumor suppressor pathway through ubiquitylation and degradation of TGF-β receptor 1, SMAD2 and SMAD4 (Komuro et al., 2004; Moren et al., 2005). WWP1 has also been shown to target p53 for proteasomal degradation (Laine and Ronai,

2007) and hence, WWP1 is suggested to function as a proto-oncogene (Chen and Matesic, 2007; Chen et al., 2008). Recent studies in *C. elegans* showed that WWP1 mediates dietary-restriction induced longevity, and loss of function of WWP1 is associated with a decline in longevity (Carrano et al., 2014; Carrano et al., 2009). Finally, WWP1 has been implicated in bone formation by negatively regulating proteins involved in osteoblast functions such Runt-related transcription factor 2 (RUNX2), the transcription factor JUNB and the chemokine receptor CXCR4 (Shu et al., 2013). A study by (Shu et al., 2013) showed that WWP1 negatively regulates osteoblast differentiation and migration based on the observation that lack of functional WWP1 in mice was associated with increased bone formation rates.

Because of its diverse functions, it is not surprising that dysfunction of WWP1 has been associated with a number of pathologies including prostate and breast carcinogenesis, neuropathology, osteoporosis and viral infections (Chen et al., 2008; Li et al., 2009; Salah et al., 2012; Shu et al., 2013; Zhi and Chen, 2012). Indeed, our previous work with a mouse model of global WWP1 overexpression demonstrated that WWP1 dysfunction also plays a role in arrhythmogenesis via its regulation of a novel target, the gap junction (GJ) protein connexin (CX) 43. Specifically, mice overexpressing WWP1 either globally or in the myocardium alone displayed a significant reduction (90%) in CX43 in the heart and die suddenly during early adulthood due to ventricular arrhythmias. In this study described here, we extend upon these observations by elucidating the molecular mechanism underlying the regulation of CX43 by WWP1.

## Gap junctions

GJs are clusters of intercellular channels that allow the direct exchange of cytoplasmic contents between adjacent cells (Goodenough and Paul, 2009). These channels are permeable to ions and small molecules less than approximately 1 kDa in size such as cAMP, glucose, ATP, glutathione and inositol 1, 4, 5-triphosphate ($IP_3$). Gap junction intercellular communication (GJIC) enables metabolic and electrical coupling of cells and plays critical roles in cellular processes such growth, differentiation and homeostasis (Goodenough and Paul, 2009). In the heart, gap junctions allow electrical impulse propagation between adjacent cardiomyocytes enabling the heart muscle to be electrically synchronized (Desplantez et al., 2007). Gap junctions are also involved in wound healing and carcinogenesis (Goliger and Paul, 1995; Leithe et al., 2006).

GJs are made up of a family of membrane proteins called connexins (vertebrates) or innexins (invertebrates). CXs are expressed in all tissue types except in differentiated skeletal muscle, erythrocytes and mature sperm cells (Nielsen et al., 2012). In humans, there are 21 known isoforms of CXs and they are designated by their approximate molecular weight in kDa. Many cell and tissue types express more than one CX isoform. For instance, keratinocytes co-express CX26, CX30, CX30.3, CX31, CX31.1 and CX43; cardiomyocytes co-express CX40, CX43, and CX45; hepatocytes co-express CX26 and CX32 (Laird, 2006; Severs et al., 2004). Co-expression of multiple connexin isoforms is believed to be a potential compensatory mechanism if mutations or loss of function arises in one of the isoforms (Gittens and Kidder, 2005). Among these isoforms, CX43 is the best described since it is expressed in the vast majority of cell types including

cardiomyocytes, keratinocytes, astrocytes, endothelial cells and smooth muscle cells among others (Laird, 2006).

Mutations in CX family members are linked to a number of diseases including deafness, skin defects and neuropathology (Gerido and White, 2004). Mutations in the gene encoding CX43 (*GJA1*) are linked with a rare, variable developmental abnormality termed as oculo-dento-digital dysplasia characterized by craniofacial defects, deafness, malformations of the limbs, skin, eye, neurological and heart defects (Debeer et al., 2005; McLachlan et al., 2005; McLachlan et al., 2008; Pizzuti et al., 2004). Mutations in *CX32* are linked with Charcot-Marie-Tooth disease which presents with progressive peripheral axon demyelination and limb weakness (Krutovskikh and Yamasaki, 2000). Hence, understanding the molecular mechanisms involved in regulating gap junction function is critical to understanding the pathophysiology of a number of different diseases.

**Life cycle of CX43**

*GJA1* is located on chromosome 6 in humans and encodes for a 382 amino acid long CX43 protein. CX43 is a four-pass integral membrane protein with two extracellular loops, an intracellular loop and the amino and carboxyl termini facing the cytoplasmic side (Fig.1.4). While the amino acid composition of the two extracellular loops is relatively conserved among the CXs, the number and composition of amino acids at the $NH_2$ and carboxyl termini are highly variable (Laird, 2006; Laird and Revel, 1990).

As an integral membrane protein, CX43 is co-translationally inserted into the endoplasmic reticulum and undergoes oligomerization in the Golgi or in the *trans*-Golgi network to form a hexameric ring like structure known as a hemi-channel or connexon. Once a hemichannel reaches the cell membrane, it docks with a hemichannel from the

adjacent cell to make a complete channel (Goodenough and Paul, 2009). A hemichannel can be homomeric (composed of a single connexin isoform) or heteromeric (composed of two connexin isoforms). Between a few hundred to thousands of these channels are deposited on the plasma membrane to form a gap junction plaque (Fig.1.4) (Ahmad et al., 1999).

GJs are dynamic structures and CX43 in gap junctions has a short half-life, ranging from one to five hours depending on the cell or tissue type (Beardslee et al., 1998; Laird et al., 1991). Newly synthesized GJ channels are deposited at the edges of the already existing gap junction plaque while the old ones are internalized from the center of the plaque (Gaietta et al., 2002; Lauf et al., 2002). GJ endocytosis involves the internalization of the plasma membranes from both cells forming the GJ channel into one of the cells as a double membrane vesicle called an annular junction or connexosome (Gumpert et al., 2008; Jordan et al., 2001) (Fig.1.5). Previous studies have indicated a role for clathrin-mediated endocytosis in GJ internalization (Fong et al., 2012; Gumpert et al., 2008). siRNA-mediated knockdown of the vesicle coating protein clathrin, clathrin-adaptor proteins AP2 and DAB2, or the GTPase DYNAMIN significantly inhibited GJ internalization (Fong et al., 2012; Gumpert et al., 2008). However the precise details of the molecular pathway involved in CX43 endocytosis and trafficking remain to be fully elucidated.

Some ultrastructural studies have suggested that , once internalized into a cell, annular junctions are further modified into single membrane bound organelles which can fuse with the early endosome (Falk and Lauf, 2001). Alternatively, internalized connexosmes can directly fuse with the lysosome or become sequestered in

autophagosomes to eventually be degraded by the lysosome (Piehl et al., 2007). Additionally, recent work has highlighted the possibility that undocked connexosomes can be endocytosed and trafficked to the early endosome (Falk et al., 2012). Thus, a variety of alternative pathways exist to account for the internalization and turnover of CX43.

**Early endosomal sorting**

Early endosomes are dynamic membrane bound compartments undergoing constant fusion with vesicles coming from the plasma membrane as well as vesicles budding off for recycling back to the plasma membrane. As such, early endosomes serve as sorting stations where endocytosed cargo arriving from the plasma membrane is directed to either the degradation or recycling pathway (Raiborg and Stenmark, 2009). This characteristic function of early endosomes is accomplished by utilizing distinct domains of the early endosomes for various functions. Cargo destined for recycling back to the plasma membrane is sequestered in the tubular subdomains of the early endosome (recycling endosomes) whereas cargo destined for the degradation pathway is captured by small vesicles that bud from the limiting membrane into the endosomal lumen to create multivesicular bodies (MVB) also known as late endosomes (Fig. 1.5). The contents of the MVB are degraded by the lysosomal hydrolytic enzymes upon fusion with the lysosome. Sorting in the early endosome is mediated in part by the endosomal sorting complex for transport (ESCRT) machinery, and ubiquitin serves as a sorting tag in this process. In particular, cargo conjugated with ubiquitin is recognized by the ESCRT machinery, facilitating its trafficking to the late endosome for lysosomal degradation (Luzio et al., 2009; Raiborg and Stenmark, 2009).

## Regulation of CX43 through post-translational modification

The role of post-translational modification in regulating the life cycle of GJs has been documented (Leithe and Rivedal, 2007). Specifically, GJs have been reported to be modified through phosphorylation, ubiquitylation, acetylation, hydroxylation and SUMOylation (Colussi et al., 2011; Kjenseth et al., 2012; Solan and Lampe, 2005; Thevenin et al., 2013). Of these, phosphorylation of CX43 has been well described, and the regulation of the life cycle of CX43 by ubiquitylation is also emerging.

## CX43 phosphorylation

Phosphorylation is a post-translational modification that affects protein hydrophobicity, charge and conformation. Phosphorylation is mediated by kinases that target serine (S), threonine (T) and tyrosine (Y) residues and is a major regulatory event both under physiological and pathological conditions. The COOH-terminus of CX43 has 21 amino acid residues that have been described to be targeted by several kinases, and CX43 phosphorylation at several sites has been reported to play a role in GJ assembly, plaque size and turnover (Solan and Lampe, 2009, 2014; Solan et al., 2007). In general, phosphorylation by AKT (PKB), PKA and casein kinase 1 (CK1) is associated with increased trafficking of CX43 to the plasma membrane and stability of CX43 within GJ (Gap junction) plaques (Dunn et al., 2012; Solan and Lampe, 2014). Specifically, phosphorylation of CX43 by PKA at S364, S365, S369, and S373 has been reported to increase GJIC and stabilize GJ plaques (Solan et al., 2007). CK1 phosphorylates CX43 on S325, S328 and S330 and its inhibition *in vivo* results in accumulation of connexons on the plasma membrane but reduction in the overall size of GJ plaques (Cooper and Lampe, 2002) suggesting a role for CK1 phosphorylation in GJ channel assembly. Phosphorylation of CX43 by CDC2 on S255 and S262 has been associated with down

regulation of GJIC through increased internalization of CX43 (Laird, 2005; Laird et al., 1991; Lampe and Lau, 2004).

Several *in vivo* stimuli such as wounding and ischemia have been associated with the induction of CX43 phosphorylation and internalization. CX43 is highly expressed in the skin and plays a primary role in the early stages of wound healing. Upon skin wounding, CX43 undergoes phosphorylation and subsequent internalization with increased keratinocyte migration to the site of wounding (Goliger and Paul, 1995). Similarly, during acute ischemia, CX43 undergoes increased phosphorylation by PKC at S368 and dephosphorylation at the CK1 sites. This altered phosphorylation profile is followed by increased CX43 internalization and lateralization of the channels from the intercalated discs (sites of end-to-end joining of cardiomyocytes) to the lateral membrane of the cardiomyocytes (Solan and Lampe, 2009, 2014; Solan et al., 2007; Tanguy et al., 2000), a condition termed GJ remodeling. GJ remodeling, in turn, alters electrical impulse propagation and creates a substrate for arrhythmia initiation (Saffitz et al., 2007).

*In vitro*, exposure of cells to tumor promoting agent phorbol 12-myristate 13-acetate (PMA), which is an analogue of the second messenger diacylglycerol (DAG), or to epidermal growth factor (EGF) induces cascades of CX43 phosphorylation events mediated mainly by MAPK, SRC and PKC kinases (Leithe and Rivedal, 2004b); (Sirnes et al., 2009; Sirnes et al., 2008). Phosphorylation of CX43 by PKC at S262 and S368 and by MAPK at S255 and S279/282 has been shown to induce CX43 internalization and increased CX43 ubiquitylation (Leithe and Rivedal, 2004b; Sirnes et al., 2009; Sirnes et al., 2008). Interestingly, it has been noted that enhanced CX43 phosphorylation is

associated with increased ubiquitylation, suggesting possible cross talk between these post-translational pathways (Laird, 2005; Laird et al., 1991).

**CX43 ubiquitylation**

Several lines of evidence indicate that CX43 undergoes ubiquitylation (Fykerud et al., 2012; Girao et al., 2009; Hertzberg et al., 1996; Leithe and Rivedal, 2004b). Tumor promoting agents EGF and PMA enhance CX43 phosphorylation, which, in turn, is associated with increased recruitment of ubiquitin to the plasma membrane (Leithe and Rivedal, 2004a, c). The first E3 ubiquitin ligase identified to target CX43 was NEDD4 (Leykauf et al., 2006). NEDD4 binds the COOH-terminal PY motif of CX43 causing a multi-mono-ubiquitylation of CX43 and subsequent internalization (Girao et al., 2009; Leykauf et al., 2006). Co-immunoprecipitation studies showed the interaction of CX43 with one of the components of the endocytic machinery, EPS15. NEDD4-mediated ubiquitylation of CX43 was required for this interaction, as siRNA mediated knockdown of *NEDD4* resulted in a disruption of this association (Girao et al., 2009). Furthermore, this interaction was dependent on the ubiquitin interaction motif (UIM) of EPS15 and mutations in this domain also abrogated the interaction of CX43 and EPS15 (Girao et al., 2009). The role of NEDD4 mediated ubiquitylation on CX43 endocytosis was further corroborated by siRNA knockdown of both *NEDD4* and *EPS15* which resulted in the stabilization of CX43 on the plasma membrane (Girao et al., 2009). Recent reports have identified two additional E3 ligases, SMURF2 and TRIM21, which can also target CX43 for ubiquitylation (Chen et al., 2012; Fykerud et al., 2012). The HECT E3 ligase SMURF2, which is a member of the NEDD4 family of E3 ligases, was found to target CX43 on the membrane, thus helping to regulate its internalization (Fykerud et al., 2012).

siRNA-mediated knockdown of *SMURF2* resulted in increased amounts of CX43 on the plasma membrane (Fykerud et al., 2012). The RING E3 ligase, TRIM21, was found to co-immunoprecipitate with CX43 although the consequence of this interaction has yet to be determined (Chen et al., 2012). Even though it has been reported that at least two different E3 ligases can target CX43 and promote its internalization, none of these events has been associated with a change in CX43 turnover, suggesting that additional E3 ligases might be involved. Based on our observation that transgenic mice overexpressing WWP1 showed a significant reduction in CX43, we hypothesize that WWP1 is the E3 ligase involved in CX43 turnover and that it acts on internalized CX43 within the early endosome.

In summary, GJIC plays a critical role in regulating cellular processes during development and differentiation and in maintaining homeostasis. Dysregulation of GJs is implicated in various pathologies including cardiac disease, neuropathologies, skin diseases, cataracts, bone defects and carcinogenesis (Debeer et al., 2005; Gerido and White, 2004; Goliger and Paul, 1995; Laird, 2006). Hence, GJ function is tightly regulated through different mechanisms including phosphorylation and ubiquitylation (Fykerud et al., 2012; Girao et al., 2009; Laird, 2005; Lampe and Lau, 2004). In this study we identify the HECT E3 ubiquitin WWP1 as a novel regulator of CX43 turnover and GJIC.

**Table 1. 1 The NEDD4 family of E3 ubiquitin ligases**

| E3 ligase | Substrate | References |
|---|---|---|
| NEDD4 | ENaC, PTEN, IGF-IR, p63, VEGF-R2, Cbl-b, EPS15, HRS. | (Snyder, 2005; Staub et al., 1996) |
| NEDD4-2/NEDD4L | ENaC, TrKA, TBR1, SMAD2, SMAD4, EPS15 | (Eaton et al., 2010; Kamynina and Staub, 2002) |
| WWP1/ Tiul1 | TBR1, SMAD2, SMAD4, KLF2, KLF5, RUNX2, p53, p63, ERB4, EPS15 | (Chen and Matesic, 2007; Li et al., 2009; Moren et al., 2005; Zhi and Chen, 2012) |
| WWP2 | OCT4, ENaC | (Eaton et al., 2010) |
| AIP4/ITCH | NF-E2, JunB, c-Jun, p63, p73, RNF11, Cbl, EPS15, Hrs, CXCR4, Notch, $CFLIP_L$, HEF1, | (Chen and Matesic, 2007; Lin and Mak, 2007; Melino et al., 2008) |
| SMURF1 | MEKK2, RUNX2, RUNX3, SMAD1-5, RhoA | (Cao and Zhang, 2013; David et al., 2013) |
| SMURF2 | TβR1, SnoN, Smad1, 2, 4, 5, RUNX2, RUNX3, RNF11 | (David et al., 2013; Ogunjimi et al., 2005) |
| HECW1/NEDL1 | SOD1, DVl1 | (Miyazaki et al., 2004) |
| HECW2/NEDL2 | P73 | (Miyazaki et al., 2003) |

Table 1 Adopted from (Chen and Matesic, 2007).

**Table 1.2 List of WWP1 targets**

| **Substrate** | **Function** |
|---|---|
| p63, p53, KLF5 | Apoptosis |
| SMAD2, TβR1, SMAD4 | TGFβ signaling |
| EPS15, RNF11, ERB4 | EGF signaling |
| GAG | Virus budding |
| JUNB, RUNX2 | Bone differentiation |
| SPARTIN/SPG20 | Neurological disorders |

## 1.2. FIGURES

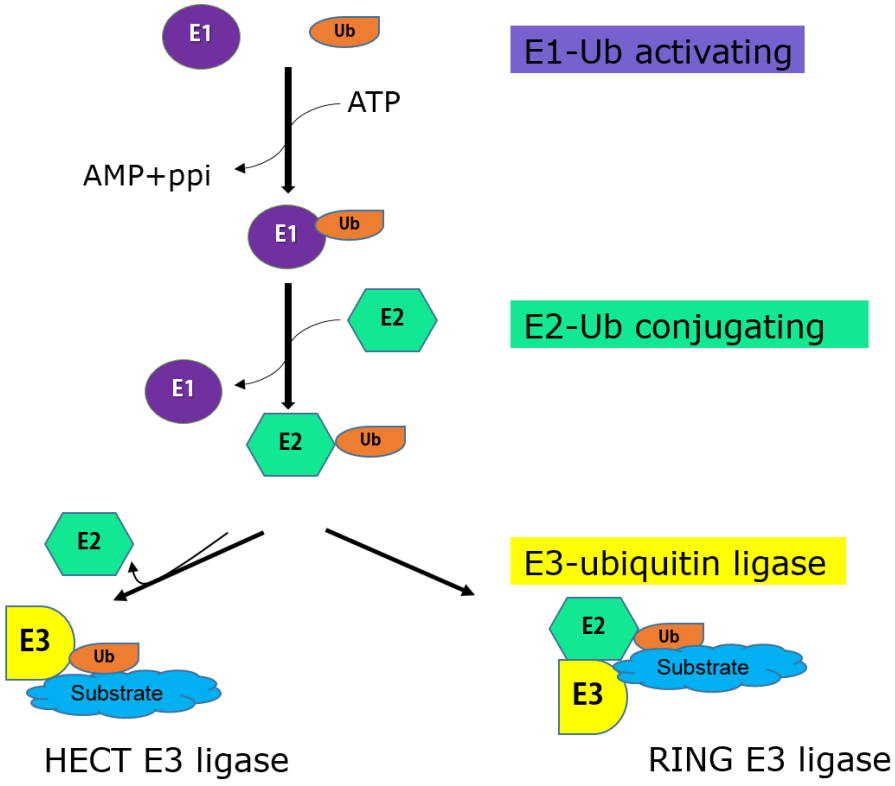


Figure 1.1 The ubiquitylation cascade. The ubiquitylation pathway involves the sequential activity of three enzymes. The ubiquitin activating enzyme (E1) activtes ubiqutin in an ATP dependent manner. The activated ubiquitin is transferred to the ubiquitin conjugating enzyme (E2). The E3 ubiquitin ligase then recruits substrates and the activated ubiquitin is either directly transferred to the substrate when HECT E3 ligases are involved or indirectly in the case of RING E3 ligases.

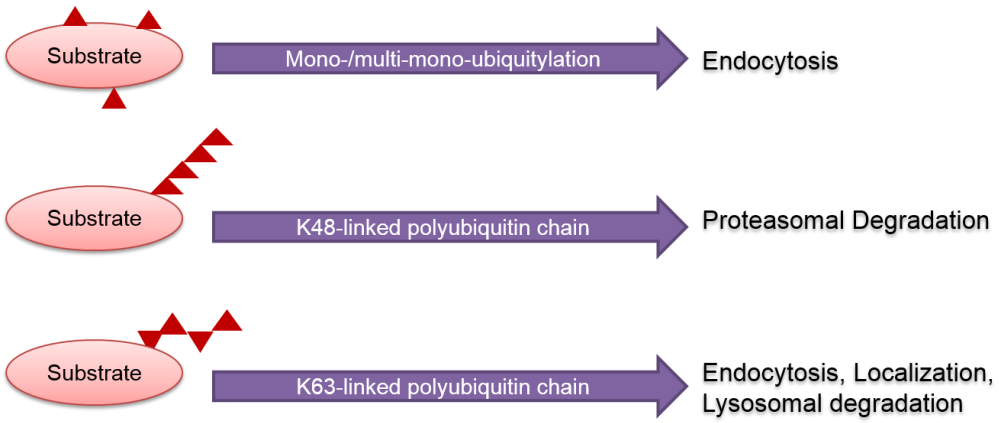


Figure 1.2. The type of ubiquitylation determines the fate of targeted substrates. The attachment of a single ubiquitin (mono-ubiquitylation) or multiple ubiquitin molecules (multi-mono ubiquitylation) is associated with endocytosis. K48-linked polyubiquitin chains are associated with proteasomal degradation whereas K63-linked polyubiquitin chains are associated with changes in subcellular localization, signaling and lysosomal degradation.

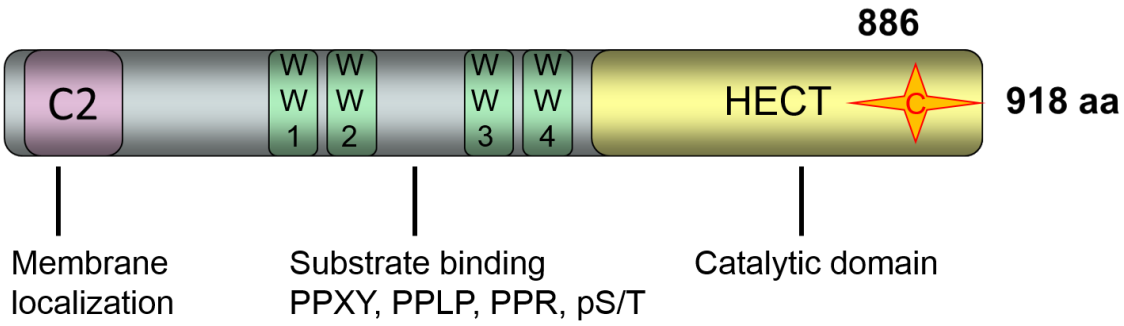


Figure 1.3. A schematic diagram showing the functional and structural domains of the WWP1 protein. The mouse WWP1 protein is 918 amino acids long and has three structural motifs. The C2 domain at the $NH_2$- terminus binds membrane phospholipids. The 4 tandem WW domains bind proline rich motifs in substrates. The COOH-terminal HECT catalytic domain has a highly conserved cysteine (C) residue at the active site (C886) that is required for its ligase activity.

A

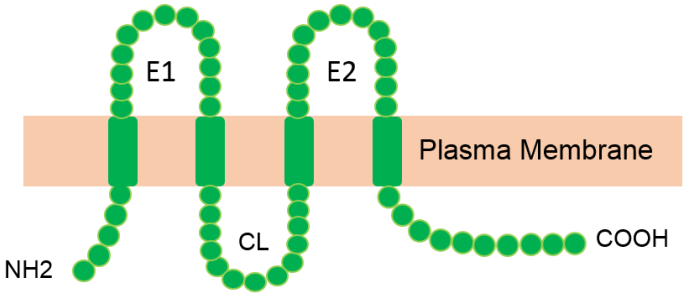


B

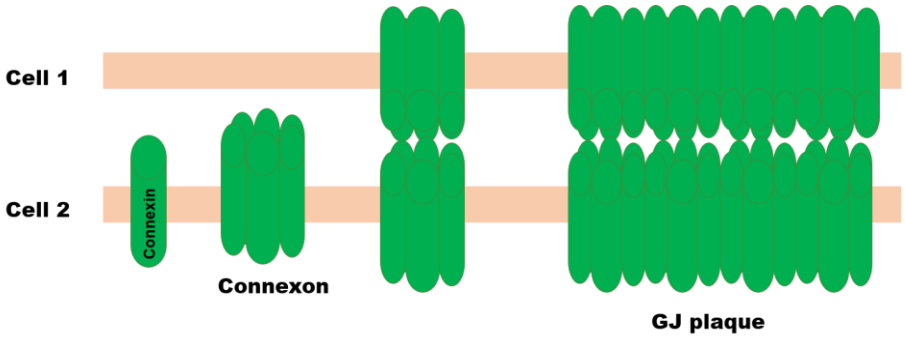


Figure 1.4 GJ assembly. GJ channels are composed of connexins. A. Connexins are four pass integral membrane proteins with two extra cellular loops (E1 and E2) and a cytoplasmic loop (CL). B. Six connexin molecules oligomerize to make a ring-like half channel termed a connexon. A connexon from one cell docks head-on with a connexon from an adjacent cell to form a full channel. Between a few hundred to thousands of these channels are deposited on the plasma membrane to form a GJ plaque.

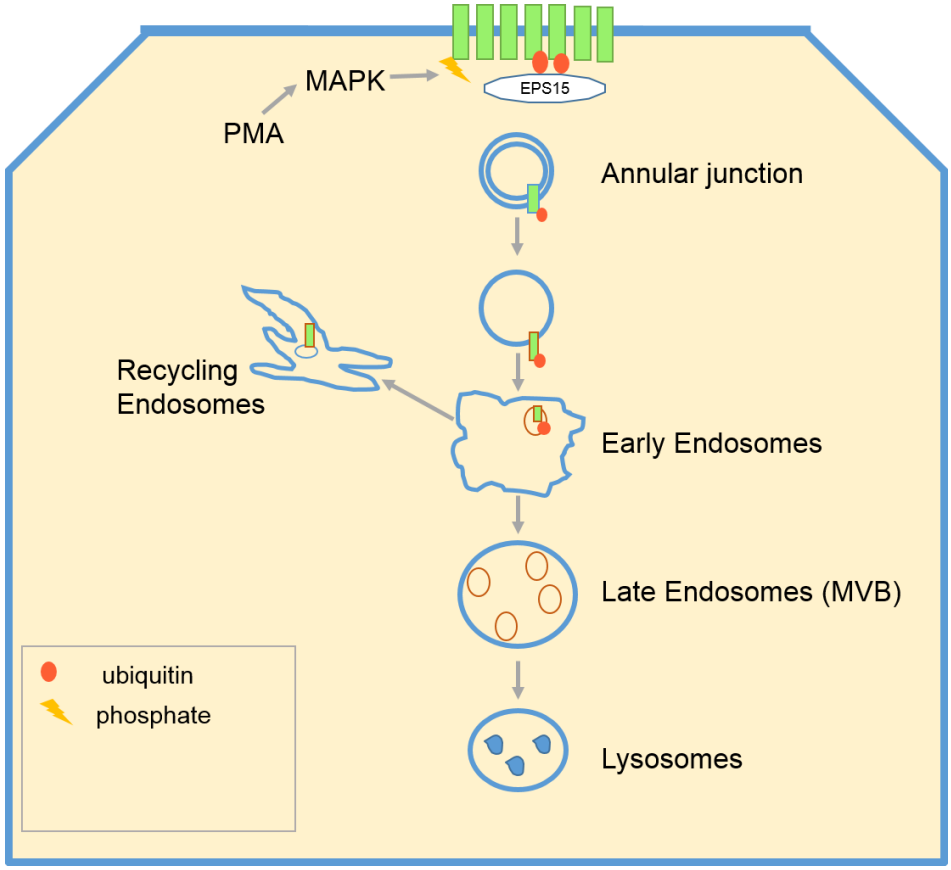


Figure 1.5 Mechanism of GJ endocytosis. GJs are endocytosed from the plasma membrane through the clathrin-mediated endocytosis (CME) pathway. Both membranes joined by the gap junctions are endocytosed into one of the cells to form a double membrane structure termed an annular junction. The annular junctions are then processed into single membrane vesicles which later fuse with the early endosome. Early endosomes act as sorting stations. Cargo proteins destined for degradation are incorporated into intraluminal vesicles (ILVs) in the formation of late endosomes (MVB). Late endosomes fuse with the lysosome and their contents are degraded by the lysosomal enzymes.

# CHAPTER TWO

## WWP1 Mediates K27- and K29-Linked Polyubiquitylation of CX43

## 2.1. INTRODUCTION

GJs are highly dynamic structures with cells constantly internalizing and assembling these channels. Unlike other integral membrane proteins, the GJ-forming protein CX43 is highly labile with a half-life ranging between one and five hours depending on the cell and tissue type considered (Beardslee et al., 1998; Laird, 2005). However, the molecular mechanisms regulating GJ turnover have not been exhaustively examined. Understanding the molecular mechanisms and pathways involved in GJ regulation is a critical first step in finding therapeutics for pathologies arising due to GJ dysregulation.

Mounting evidence supports the role of post-translational modification in GJ assembly and turnover. In particular, the role of phosphorylation on CX43 half-life has been well described. In fact, CX43 is phosphorylated just after translation and some of these modifications have been reported to be critical in proper trafficking of CX43 to the plasma membrane, in channel assembly, as well as endocytosis from the plasma membrane (Laird, 2005; Laird et al., 1991; Lampe and Lau, 2004). Further, the phosphorylation status of CX43 changes in response to physiological and environmental stimuli such as acute ischemia and wounding. This altered phosphorylation is followed by increased CX43 internalization and turnover (Solan and Lampe, 2009, 2014; Solan et al., 2007; Tanguy et al., 2000). *In vitro*, exposure of cells to PMA and EGF induces cascades of CX43 phosphorylation events mediated mainly by MAPK, SRC and PKC kinases (Leithe and Rivedal, 2004b); (Sirnes et al., 2009; Sirnes et al., 2008). Interestingly, the increased phosphorylation and endocytosis of CX43 was associated

with increased CX43 ubiquitylation and turnover suggesting a role for ubiquitylation in CX43 turnover.

Previous studies have shown that CX43 is ubiquitylated. Specifically, immunoprecipitation of CX43 followed by immunoblotting using anti-ubiquitin antibodies demonstrated the existence ofubiquitylated forms of CX43 (Leithe and Rivedal, 2007). The HECT E3 ligase NEDD4 was the first E3 ligase identified to bind and ubiquitylate CX43 (Girao et al., 2009; Leykauf et al., 2006). NEDD4 has three tandem WW domains (WW1, WW2, and WW3) in humans and binds the COOH-terminal proline rich (PPXY) motif of CX43 through WW2 (Leykauf et al., 2006). NEDD4-mediated ubiquitylation seems to be important in the endocytosis of CX43. In particular, NEDD4-mediated ubiquitylation of CX43 has been shown to enhance the binding of the endocytic protein EPS15 to CX43. Deletion of the ubiquitin interacting (UIM) of EPS15 abrogated this interaction, suggesting there is ubiquitin-dependent recruitment of EPS15 (Girao et al., 2009). Furthermore, siRNA-mediated knockdown of *NEDD44* in African green monkey kidney fibroblast like (Cos-7) cells as well as siRNA knockdown of *Eps15* in normal rat kidney epithelial (NRK) cells was associated with increased levels of CX43 at the plasma membrane, confirming a role for NEDD4-mediated ubiquitylation in the internalization of CX43 (Girao et al., 2009). However, NEDD4 knockdown did not result in a change in the total CX43 protein level ((Leykauf et al., 2006), suggesting that additional ubiquitylation events might be required for turnover of CX43 by the lysosome.

The HECT E3 ligase SMAD regulatory factor 2 (SMURF2) has also recently been reported to regulate CX43 endocytosis. The study showed an interaction between

CX43 and SMURF2 in a rat epithelial cell line, IAR20 (Fykerud et al., 2012). siRNA mediated knockdown of endogenous *Smurf2* in IAR20 cells resulted in increased CX43 at the membrane and a subsequent increase in GJIC, revealing a role for SMURF2 in CX43 internalization (Fykerud et al., 2012). Finally, proteomic studies using mass spectrometry showed the association of CX43 with the RING E3 ligase, TRIM21, in rat glioma cells transfected with CX43 (C6-CX43); however, the role of this association on the regulation of the CX43 life cycle has not yet been described (Chen et al., 2012).

Recent work from our lab suggests that CX43 may also be targeted by the HECT E3 ligase WWP1, a member of the NEDD4 subfamily of E3 ligases. In particular, we found that mice overexpressing WWP1 had a significant reduction (~80%) in CX43 protein in the heart (Fig 2.1). Here, we build upon this observation by unraveling the molecular mechanisms by which WWP1 regulates CX43 and GJIC *in vivo* using an established tissue culture system (*i.e.,* HeLa and 293T cells). These cells were chosen for a variety of reasons. Specifically, it has been reported that CME is an important component of CX43 endocytosis in a HeLa-based model system (Gumpert et al., 2008). Both assembly of function GJ as well as endocytosis of these structures has been described in HeLa cells stably transfected with CX43 (Gumpert et al., 2008; Piehl et al., 2007). In addition, because HeLa cells are not known to express any CX isoforms (Gilleron et al., 2011), cell lines stably transfected with just one isoform are ideal for the study of homomeric, homotypic GJs. Further, 293T cells have been described to mediate trafficking of exogenously expressed CX43 in a similar manner. In particular, siRNA-mediated knockdown of *EPS15,* a component of the CME machinery, in 293T cells resulted in the accumulation of CX43 on the membrane (Girao et al., 2009),

suggesting that a common mechanism for CX43 trafficking exists in both cell types cell types. Using this model cell culture system, we showed that WWP1 co-immunoprecipitates with CX43 and the co-immunoprecipitation was enhanced in the presence of PMA. We determined that this interaction was dependent upon an intact PY motif in CX43. The interaction between WWP1 and CX43 promoted the K27- and K29-linked polyubiquitylation of CX43 as a dead ligase version of WWP1 failed to target CX43. Thus, this represents the first report of this unconventional polyubiquitin post translational modification of a GJ protein.

## 2.2. MATERIALS AND METHODS

### Cell Culture

Human embryonic kidney (HEK) 293 T cells were kindly provided by Dr. Dan Dixon of the University of South Carolina. Human cervical carcinoma cells (HeLa) cells were purchased from ATCC. Both cell lines were maintained in culture in Dulbecco's Modified Eagle Medium (DMEM) supplemented with 10% Fetal Bovine Serum (FBS) plus 1% penicillin/streptomycin in 5% $CO_2$, and 37°C growth incubator. Transfections were done with JetPRIME (polyPLUS) and Lipofectamine 2000 reagent (Invitrogen) according to the manufacturer's recommendations. HeLa cells stably transfected with CX43 (HeLa-CX43) were generated by transfecting the CX43 expression vector, pCDNA3.1-CX43, into HeLa cells using Lipofectamine reagent (Invitrogen) and selecting for transfected cells using 400 mg/mL of G418. Western blot analysis and immunofluorescence staining was performed to confirm CX43 expression and formation of gap junctions. The function of gap junctions was also assessed using a dye

travel/scrape loading assay and clones with functional gap junctions based on dye transfer assay were selected.

**Plasmids**

The CX43 expression plasmid pCDNA3.1-CX43, was kindly provided by Dr. Alan Lau (University of Hawaii Cancer Center). The WWP1 expression plasmid pCMV-Tag3-Myc-Cherry-WWP1 was kindly provided by Dr. Ceshi Chen (Kunming Institute of Zoology, Chinese Academy of Sciences). The XhoI/ApaI fragment containing the C886S mutation was cloned from Myc-C886S to pCMV-tag3-Myc-Cherry-WWP1 to create pCMV-tag3-Myc-Cherry-C886S. The following variants of ubiquitin expression plasmids were purchased from Addgene and have been described before (Lim et al., 2005; Lim et al., 2006; Livingston et al., 2009): pRK5-HA-Ub-WT, pRK5-HA-Ub-K0, pRK5-HA-Ub-K6, pRK5-HA-Ub-K11, pRK5-HA-Ub-K27, pRK5-HA-Ub-K29, pRK5-HA-Ub-K33, pRK5-HA-Ub-K48, and pRK5-HA-Ub-K63. A PY motif mutant form of CX43 was generated by changing a conserved proline at residue 283 to a leucine (CX43-P283L) using the QuickChange site-directed mutagenesis kit according to the manufacturer's instructions (Agilent Technologies).

**Co-immunoprecipitation assay**

293T cells were transfected with JetPRIME reagent (polyPLUS). A day after transfection, cells were treated with 100 ng/mL PMA. Forty-eight hours post transfection, cells were rinsed with chilled 1X PBS and lysed with non-denaturing lysis buffer (50 mM Tris-Hcl, pH 7.5, 150 mM NaCl, 0.5% Triton X-100 supplemented with cocktail protease inhibitors plus EDTA, 10 mM iodoacetamide, 2 mM sodium orthovanadate). 500 µg of

cell lysate was incubated with anti-CX43 antibody (Zymed, 71-0700) overnight followed by incubation with 30 µL protein A/G agarose beads (Santa Cruz, SC-2003) for 3 hrs. Immunoprecipitated proteins were eluted with 2X Laemmli sample buffer, boiled for 5 min at 95°C and separated by SDS-PAGE. Samples were transferred to PVDF membrane (BioRad) and probed with the following antibodies: anti-CX43 (Sigma, C6219) anti-HA (Sigma, clone HA-7), anti-Myc (Santa Cruz, 9E10).

**Ubiquitylation assay**

293T cells were transfected with CX43, either Myc-WWP1 or Myc-C886S, and HA-Ub. Forty-eight hours post transfection, cells were treated with 100 ng/mL of PMA for one hour and were subsequently rinsed with cold 1X PBS and then lysed with Triton X-100 non-denaturing lysis buffer (50 mM Tris-Hcl, pH 7.5, 150 mM NaCl, 0.5% Triton X-100, supplemented with cocktail protease inhibitors plus EDTA, 10 mM iodoacetamide, 2 mM sodium orthovanadate). 500 µg of cell lysate was incubated with 1 µg of anti-CX43 antibody (Invitrogen, 71-0700) overnight. Protein-antibody immuno-complex was formed by adding 30 µL of protein A/G agarose beads. The immunoprecipitated protein complex was eluted with 40 µL of 2X Laemmli sample buffer, boiled for 5 min at 95°C and run on 4-15% TGX polyacrylamide gel (Bio-Rad). The samples were blotted to PVDF membrane and blocked using a blocking buffer (5% non-fat dry milk in TBST (Tris-Buffered Saline plus Tween-20). The blot was probed using the following antibodies: anti-HA (Sigma, HA-7), anti-CX43 (Sigma, C6219) and anti-Myc antibodies (Santa Cruz, 9E10).

**Western blotting**

293T cells were harvested using Triton X-100 lysis buffer (150 mM NaCl; 50 mM Tris-HCl, pH 7.5; 0.5% Triton X-100 supplemented with cocktail protease inhibitors plus EDTA, 2 mM sodium orthovanadate, and 10 mM iodoacetamide). 25-50 µg of protein was loaded and separated on a 4-15% gradient polyacrylamide gel, transferred to PVDF membrane (Bio-Rad), and blocked for 1 hour using 5% non-fat dry milk in TBST followed by probing with primary antibodies for 16 hours at 4°C. Images were taken using Fluorchem E Chemiluminescent Western blot Imaging System (ProteinSimple) and quantification of protein intensity was done using AlphaView imaging software.

**Immunofluorescence staining**

HeLa-CX43 cells grown on coverslips were transfected using either mCherry-WWP1 or mCherry-C886S plasmids. 48 hrs post transfection, cells were treated with 100 ng/mL PMA for 1 hr. Cells were rinsed with PBS and fixed in 4% PFA for 15 min at room temperature, rinsed 3X with PBS and then treated with a blocking buffer (5% normal goat serum, 1% BSA and 0.3% Triton X-100 in PBS) for 1 hr at room temperature. Cells were stained using primary antibodies overnight at 4°C followed by incubation with fluorophore conjugated $F(ab')_2$ fragment secondary antibodies (Jackson Immunoresearch) as indicated. Cover slips were mounted using Fluoro-Gel mounting media (Electron Microscopy Sciences). Images were acquired using the 100X objective of a Leica DMI6000B microscope with a Hamamatsu Camera C10600.

### Statistics

Statistical analysis of quantitative data were calculated and plotted using Prism software (GraphPad). All experiments were performed at least three independent times with similar results. Student's t-test and one-way ANOVA were used to test for statistical significance and p-values ± 0.05 were considered significant.

## 2.3. RESULTS

### WWP1 co-immunoprecipitates with CX43

The role that ubiquitylation plays in CX43 turnover has only begun to emerge. Recent studies have identified two members of the NEDD4 subfamily of E3 ligases, NEDD4 and SMURF2, as regulators of the endocytosis of CX43 (Fykerud et al., 2012; Girao et al., 2009; Leykauf et al., 2006). These studies showed that the internalization of CX43 was enhanced by its interaction with and subsequent ubiquitylation by both ligases. However, neither of these E3 ligases induced CX43 turnover. Based on these observations we hypothesized that WWP1, which has been previously reported to localize predominantly to the early endosome (Zhi and Chen, 2012) targets endocytosed CX43 in the early endosome rather than at the plasma membrane.

To investigate whether WWP1 interacts with CX43, a co-immunoprecipitation (co-IP) assay was performed using 293T cells co-transfected with CX43 and either Myc-WWP1 or a mutant version of WWP1 that lacks ubiquitin ligase activity (Myc-C886S) due to a cysteine to serine mutation at its active site. Our data showed the interaction of CX43 with both WWP1 and C886S, indicating that the ligase activity is not required for the interaction of these two proteins (Fig. 2.2A). Immunoprecipitation of cell lysates

expressing both CX43 and WWP1 with a control rabbit polyclonal IgG antibody as well as immunoprecipitation of untransfected cell lysates with anti-CX43 antibody resulted in no detectable WWP1, confirming the specificity of the interaction (Fig. 2.2A, lanes 3, 6, 7). Previous studies have demonstrated that exposure of cells to PMA in culture induces endocytosis and increased ubiquitylation of CX43 (Sirnes et al., 2008). In an effort to determine the effect of PMA on the interaction of CX43 on WWP1, the co-immunoprecipitation was repeated in transfected 293T cells stimulated with PMA for 30 min. Cell lysates were harvested after six hours of washout period followed by co-IP assay. Our data showed that, upon PMA exposure, there was a significant increase in the amount of CX43 detected in the cell lysate as well as a corresponding increase in the level of WWP1 that co-immunoprecipitated with CX43 (Fig. 2.2A).

**The interaction of CX43 with WWP1 is dependent upon an intact PPXY motif in CX43**

E3 ubiquitin ligases have protein-protein interaction domains that allow for specific binding to target proteins, thus providing substrate specificity. WWP1 has 4 tandem WW domains that have affinity for proline-rich modules such as PPXY, PPLP and phosphorylated serine and threonine (pS/T) (Fig. 1.3). CX43 possesses a PPXY motif on its COOH-terminal cytoplasmic tail, and this region has been reported to bind the WW domain of the E3 ligase NEDD4 (REFERENCE). In an effort to determine whether the interaction of WWP1 with CX43 is dependent on the PPXY motif, site-directed mutagenesis was used to introduce a proline to leucine substitution at residue 283 of CX43 (CX43-P283L). When PMA stimulated 293T cells were co-transfected with CX43-P283L and Myc-WWP1 and the co-immunoprecipiation of PY mutant CX43 and

WWP1 was examined, a dramatic reduction in the level of WWP1 pulling down with CX43-P283L was noted (Fig. 2.2B). These data demonstrated that the co-immunoprecipitation of WWP1 with CX43 is dependent on an intact PPXY motif.

**Co-localization of CX43 and WWP1 in the early endosomes**

As increased interaction between CX43 and WWP1 was evidenced upon endocytosis-promoting PMA stimulation (Fig. 2.2A) and since previous studies have reported that WWP1 localizes to the early endosome (Zhi and Chen, 2012), we hypothesized that WWP1 might interact with CX43 in the early endosome. To test this hypothesis, HeLa cells stably expressing CX43 (HeLa-CX43) were transfected with mCherry-tagged WWP1. Forty-eight hours following transfection, cells were treated with 100ng of PMA for one hour, then fixed and immunofluorescently stained with anti-CX43 and anti-EEA1 antibodies. Co-localization of WWP1, CX43, and the early endosome marker EEA1 was visualized as white overlap of the three fluorochromes. Our data showed the co-localization of CX43 and mCherry-WWP1 in the early endosomes (Fig. 2.3), demonstrating that WWP1 can associate with internalized CX43 in a subdomain of the early endosome.

**WWP1 mediates ubiquitylation of CX43**

Given the interaction of WWP1 and CX43 proteins, we next examined whether WWP1 could target CX43 for ubiquitylation *in vivo*. This was accomplished by co-transfecting 293T cells with CX43, HA-tagged Ubiquitin (HA-Ub) and either Myc-WWP1 or Myc-C886S. Ubiquitylation of CX43 was assessed by immunoprecipitating with anti-HA antibody and then immunoblotting with anti-CX43 antibody to look for ubiquitylated forms of CX43. The conjugation of a single ubiquitin moiety adds about 8

kDa to the molecular weight of a substrate, causing a shift in migration on SDS page. Our data showed that CX43 is conjugated with ubiquitin and this was indicated as an increase in CX43 molecular weight to form a ladder-like or smear on the blot that ranged between 50 to 100 kDa in size (Fig. 2.4A). Our data also showed this modification to be dependent on the ligase activity of WWP1 as the catalytically inactive form of WWP1 showed dramatically reduced ubiquitylation activity (Fig.2.4A, lane 2). In order to confirm the specificity of WWP1-mediated ubiquitylation of CX43 and to rule out the possibility of an unknown ubiquitylated protein being pulled down with CX43, a reciprocal immunoprecipitation was performed using an anti-CX43 antibody followed by immunoblotting with an anti-HA antibody. Our reciprocal IP data confirmed that WWP1 directly ubiquitylates CX43 and this modification was dependent on the ligase activity of WWP1 (Fig. 2.4B). In addition, our data revealed that overexpression of WWP1 resulted in a substantial reduction in CX43 protein in the input suggesting that WWP1 is causing CX43 turnover (Fig. 2A & B).

**WWP1 promotes K27- and K29-linked polyubiquitylation of CX43**

The ladder-like appearance on our ubiquitylation data could arise from the conjugation of multiple ubiquitins on different lysine residues (multi-mono-ubiquitylation) or the addition of a polyubiquitin chain. To differentiate between multi-mono and polyubiquitin conjugation of CX43, the ubiquitylation assay was repeated using a mutant HA-tagged ubiquitin (HA-K0) in which all the lysine residues were mutated to arginine so that it was rendered incapable of extending a polyubiquitin chain. Our data showed that ubiquitylation of CX43 was highly reduced upon expression of the mutant Ub (HA-K0) indicating that the ladder like appearance on the SDS-PAGE was in

fact due to the conjugation of a polyubiquitin chain instead of multi-mono ubiquitylation on CX43 (Fig. 2.5A, lane2).

To determine the type of polyubiquitin linkage conjugated by WWP1, the ubiquitylation assay was repeated using mutant ubiquitin variants that have only one lysine residue to accept the growing chain while the rest of the lysine residues have arginine substitutions. The results indicate that WWP1 preferentially promotes the conjugation of K27- and K29-linked polyubiquitin chains on CX43 (Fig. 2.5A). Extension of the K27-and K29-linked polyubiquitin chains was dependent on the catalytic activity of WWP1, as the dead ligase was unable to promote these linkages (Fig. 2.5B).

## 2.4. DISCUSSION

In this study we demonstrated that WWP1 could co-immunoprecipitate with CX43 and this interaction was dependent on the PPXY motif of CX43, as mutations in this domain resulted in a dramatic reduction in the level of WWP1 that pulled down with CX43. However there was a small amount of co-immunoprecipitation of WWP1 with mutant CX43-P283L, which could be the result of interaction of WWP1 with the phospho-serine/threonine motifs of CX43-P283L since WW domains are known to have affinity for phosphor-S/T motifs ((Macias et al., 2002). Alternatively, it remains a formal possibility that the WW domains of WWP1 are binding to other proteins in the immunoprecipitated complex. However, co-expression of GST-tagged WWP1 with CX43 or P283L-CX43 protein followed by GST pull down assays will be necessary to rule out the above possibility.

PMA is known to induce hyperphosphorylation of CX43 followed by increased GJ endocytosis and ubiquitylation of CX43 (Leithe and Rivedal, 2004d; Rivedal and Leithe, 2005; Sirnes et al., 2008). PMA has also been reported to increase the transcription or translation of CX43 (Rivedal and Leithe, 2005). The studies described here show increased co-immunoprecipitation of CX43 with WWP1 in the presence of PMA. This could be the consequence of either more cytoplasmic CX43 being made available for interaction with WWP1 upon PMA stimulation (though endocytosis or via transcription and translation) or of increased affinity of WWP1 for phosphorylated CX43. In this study we saw interaction of WWP1 and CX43 even in the absence of PMA-induced phosphorylation, albeit to a lesser extent compared to what was observed in the presence of PMA. Considering the fact that WWP1, CX43, and EEA1 co-localize upon PMA stimulation, we suggest that the endocytosis-promoting phosphorylation of CX43 associated with PMA stimulation enhances the interaction with and subsequent ubiquitylation by WWP1, but this modification is not absolutely necessary for this interaction to occur.

Previous studies have reported that NEDD4-mediated multi-mono-ubiquitylation of CX43 enhanced EPS15-dependent internalization of CX43 (Girao et al., 2009). In contrast, when a ubiquitylation assay was performed using a mutant (K0) ubiquitin, which permits multi-mono-ubiquitin conjugation of substrates but does not allow for the formation of polyubiquitin chains, the E3 ligase WWP1, and CX43, we found no detectable ubiquitylation of CX43 suggesting that closely related family member WWP1 promotes a different kind of ubiquitylation of the same substrate and may therefore function in a separate step in the degradative phase of the CX43 life cycle. Instead,

WWP1 promoted K27- and K29-polyubiquitylation of CX43. The role of modification by such atypical polyubiquitin chains on protein function and stability is underappreciated. A study has reported the role of K29-linked polyubiquitylation of Deltex by the HECT E3 ligase ITCH. K29-polyubiquitylation of Deltex was reported to increase lysosomal trafficking (Chastagner et al., 2006). These atypical linkages have also been associate with protein aggregations in Huntington pathogenesis (Zucchelli et al., 2010).

Previously reported ubiquitylation of CX43 by both NEDD4 and SMURF2 was not associated with CX43 turnover. However, overexpression of wild type WWP1 was associated with a robust reduction in CX43 levels (Fig. 2.1 and Fig. 2.4, input), implying that WWP1-mediated ubiquitylation of CX43 promotes turnover of the substrate protein. This is seemingly at odds with a recently published study which showed that a mutant form of CX43 that has all its lysine residues substitutes with arginines behaved the same way as wild type CX43 in the presence of both proteasomal and lysosomal inhibitors (Dunn et al., 2012). In that report, the addition of proteasomal inhibitors was associated with an increase in the amount of CX43 at the plasma membrane with a corresponding increase in the intensity of a 50 kDa CX43 band on western blot (which happens to be the same size as a mono-ubiquitylated CX43). The observed increase of CX43 after proteasomal inhibition was shown to be secondary to the stabilization of AKT/PKB which directly phosphorylates CX43 to inhibit its internalization (Dunn et al., 2012). In contrast, our study showed that WWP1 promotes K27- and K29-linked polyubiquitylation of CX43. This event was greatly enhanced by PMA stimulation, which promotes MAPK- and PKC-dependent phosphorylation of CX43 on different residues, and these changes have been associated with the increased endocytosis of CX43

(Solan and Lampe, 2005). Taken together, these data suggest that CX43 is endocytosed in a WWP1-independent manner and WWP1 acts upon CX43 at the level of the early endosome.

## 2.5. FIGURES

A

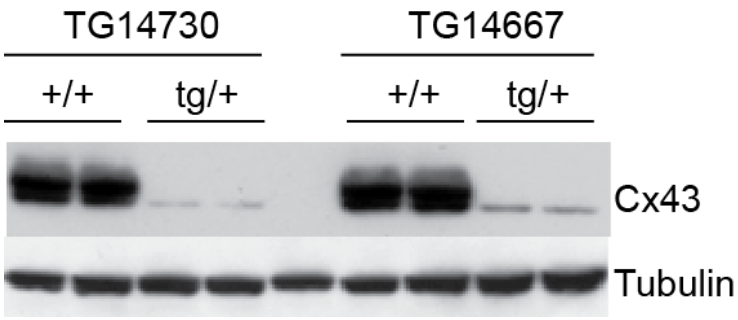


B

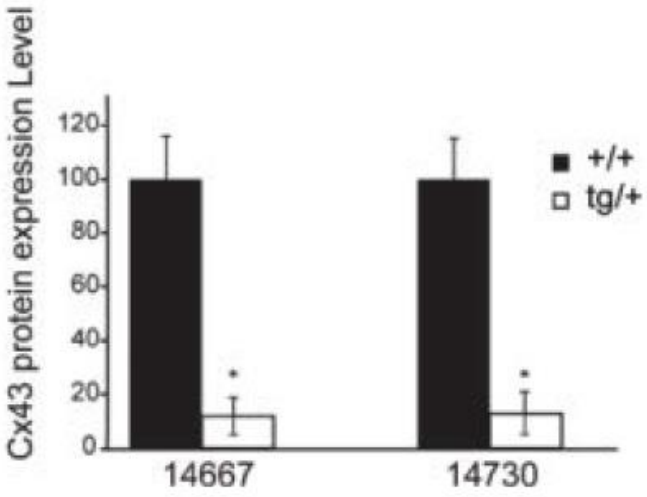


Figure 2.1 A. WWP1 overexpressing mice display reduced cardiac CX43. Western blot analysis of heart samples derived from WWP1 overexpressing transgenic mice revealed a reduction in CX43 protein compared to WT animals in two independent transgenic lines (14667 and 14730). B. Quantification of the CX43 protein level showed an eighty percent reduction in the CX43 protein level in transgenic mice compared to WT animals.

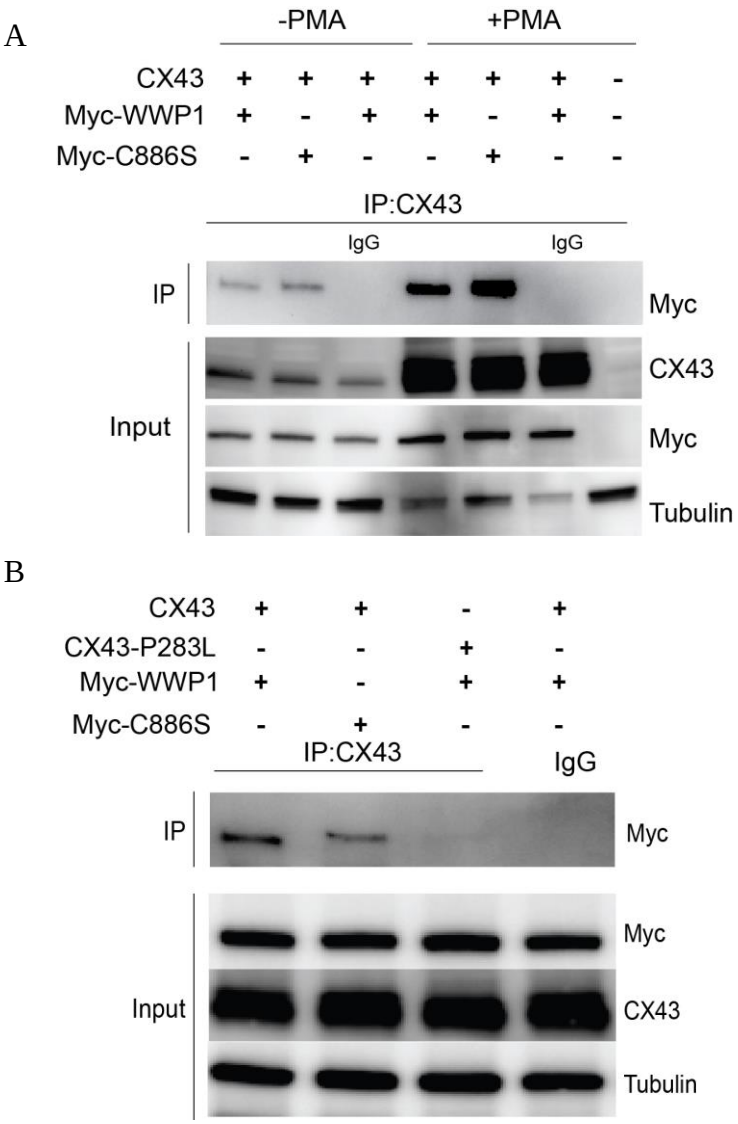


Figure 2.2 WWP1 co-immunoprecipitates with CX43 via the PPXY motif. A. 293T cells were co-transfected with CX43 and either Myc-WWP1 or Myc-C886S, immunoprecipitated using an anti-CX43 antibody, and then probed for the presence of WWP1 using an anti-Myc tag antibody. This analysis revealed the interaction of both WWP1 and mutant WWP1 (C886S) with CX43, suggesting the association is independent of the ubiquitin ligase activity of WWP1. The co-immunoprecipitation was enhanced in the presence of PMA. Shown here are representative images from three independent trials. B. The co-immunoprecipitation assay was repeated in PMA-stimulated 293T cells that were co-transfected with Myc-WWP1 or Myc-C886S and with either CX43 or a mutant CX43 (CX43-P283L) which bears a proline to leucine mutation in its PPXY motif. The mutant CX43 showed a dramatic reduction in the amount of WWP1 that was pulled down, particularly as compares to wild type CX43 (compare lanes 1 and 3 or 2 and 4). Shown here are representative images from three independent experiments.

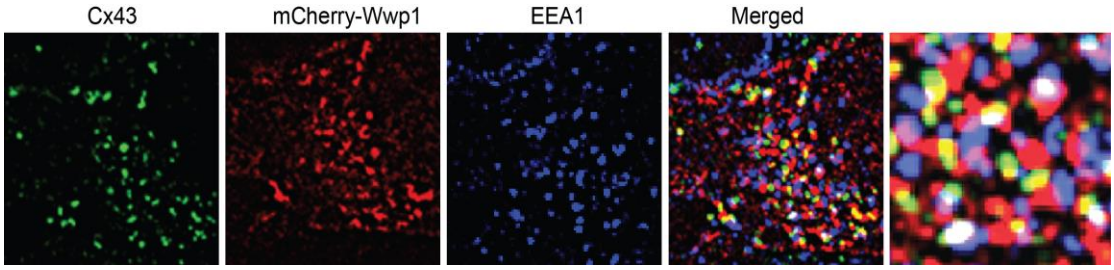


Figure 2.3 Co-localization of CX43 with WWP1 in the early endosome. HeLa-CX43 cells were transfected with mCherry-WWP1 (red) and then forty eight hours later were treated with 100 ng/mL PMA for 1 hr. Cells were fixed and immunofluorescently labelled using anti-CX43 (green) and anti-EEA1 antibodies (blue). Images were taken using Olympus IX81 (Hamamatsu C10600 camera). 2D deconvolution was performed using MetaMorph Basic to remove out of focus light. Our data showed intracellular co-localization of CX43 with WWP1 (yellow) as well as co-localization of both CX43 and mCherry-WWP1 in the early endosomes (white). Overlap of WWP1 and EEA1 is shown in magenta while overlap of CX43 and EEA1 is shown in cyan. Shown here are representative images.

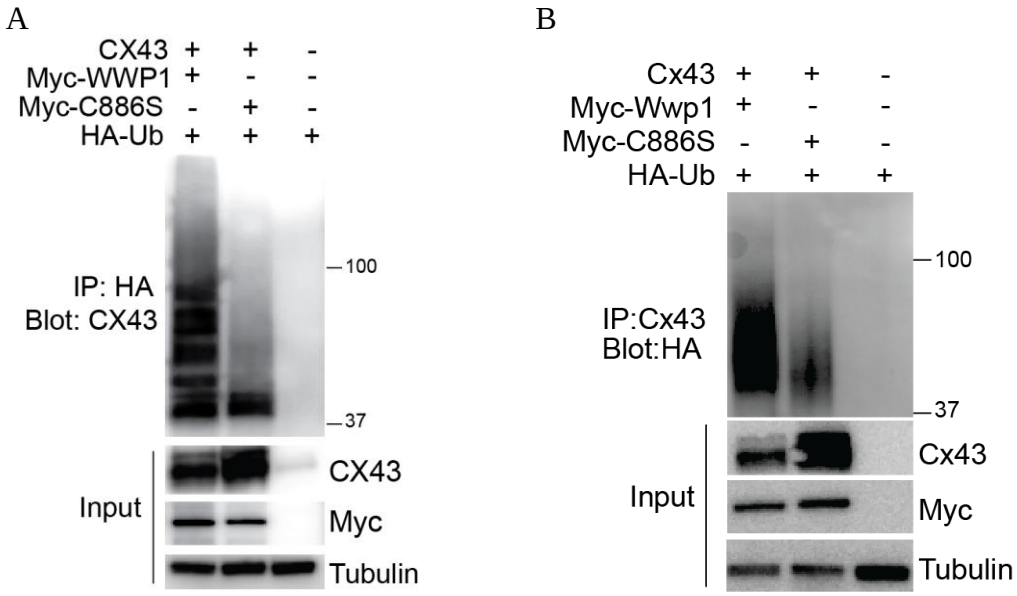


Figure 2.4 WWP1 mediates ubiquitylation of CX43. A. PMA-stimulated 293T cells were co-transfected with CX43, HA-tagged Ub and either Myc-WWP1 or Myc-C886S. Cells lysates were immunoprecipitated with anti-HA antibody and then probed with anti-CX43 antibody to detect ubiquitylated forms of CX43. WWP1 mediates ubiquitylation of CX43 as the high molecular weight ladder between 50 and 100 kDa is completely abrograted when a mutant version of WWP1 that lacks ubiquitin ligase activity was utilized. A significant reduction in the steady state level of CX43 was noted when wildtype WWP1 was overexpressed (compare input for Myc-WWP1 vs. that for Myc-C886S). B. These results were confirmed using a reciprocal immunoprecipitation assay. In particular, PMA-stimulated 293T cells were transfected with the same expression constructs as above and an immunoprecipitation for CX43 was performed followed by immunoblotting for HA-tagged ubiquitin. Again, ubiquitylation of WWP1 (in the form of a high molecular weight smear) was evidences only in the presence of WT WWP1

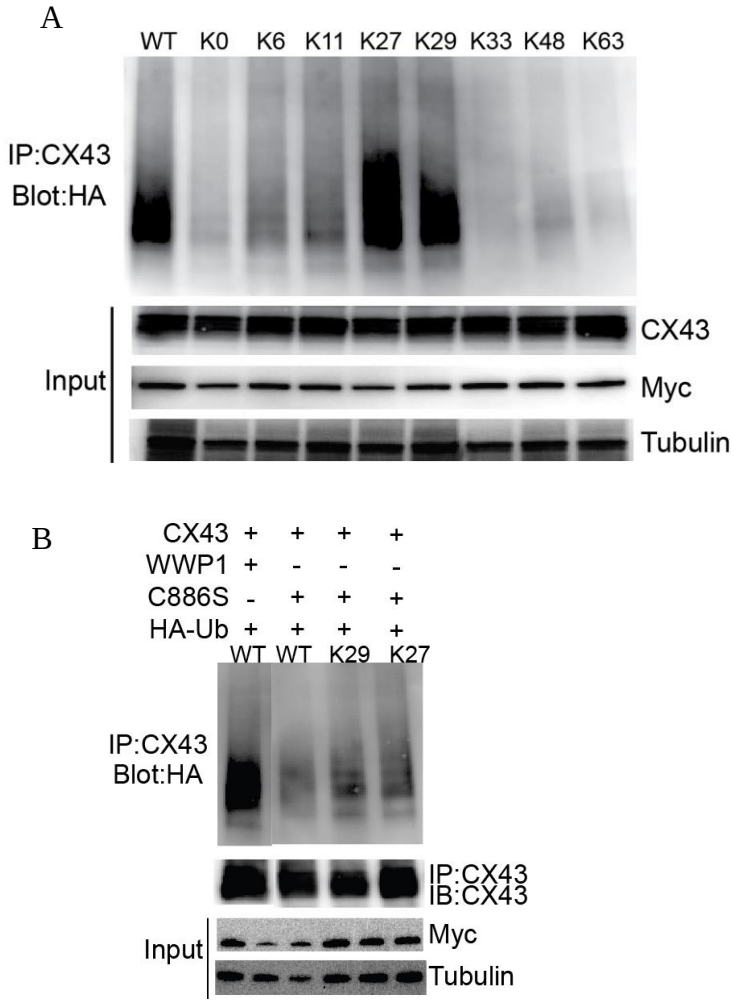


Figure 2.5 WWP1 mediates K27- and K29-linked polyubiquitylation of CX43. A. A ubiquitylation assay was performed in PMA-stimulated 293T cells by overexpressing CX43, Myc-WWP1 and one of the seven HA-tagged ubuquitin variants that have only the indicted lysine residue available to extend a polyubiquitin chain. WWP1 preferentially conjugates K27- and K29-linked polyubiqutin chains on CX43 (lanes 5 & 6). B. When PMA-stimulated 293T cells were instead transfected CX43, either Myc-WWP1 or Myc-C886S, and with the indicated version of HA-tagged ubiquitin, it was noted that K27- and K29-polyubiquitylation of CX43 was dependent on the ligase activity of WWP1.

# CHAPTER THREE

## WWP1-Mediated Ubiquitylation of CX43 Regulates CX43 Turnover and GJIC

## 3.1. INTRODUCTION

The level of GJ communication between cells is strictly regulated through multiple mechanisms, including alternations in GJ channel permeability as well as rapid channel assembly and disassembly (Laird, 2006). The ability of a solute to pass through a GJ channel depends on its net charge, size and interactions with specific CXs that constitute GJs (Goldberg, 2003; (Nielsen et al., 2012). The conductance of a GJ channel depends on the type of CX isoform from which it is assembled, and further variations in conductance are created by assembling homomeric (composed of the same type of CX) or heteromeric (composed of different CX isoforms) hemichannels (Ahmad et al., 1999). Gap junctional communication can also be regulated through channel gating, a term used to describe channel opening and closing. Channel gating is regulated by change in pH, voltage, $Ca^{2+}$ concentration, phosphorylation and protein interactions (Musil and Goodenough, 1990). In this study we focused on GJ regulation via channel turnover.

GJs are highly dynamic structures that undergo constant assembly and disassembly. Cells regulate the number of GJ channels by balancing the rate of synthesis with the turnover of CXs. CXs are characterized by their high turnover rate with constant deposition of newly formed channels at the edge of GJ plaques and endocytosis of already existing channels from the center of those plaques (Musil and Goodenough, 1990). The high turnover rate of GJs has been suggested to be a mechanism of regulating GJIC. It is hypothesized that ubiquitylation may be one mechanism for facilitating the rapid turnover of GJs.

Although previous studies have identified the E3 ligases NEDD4 and SMURF2 as regulators of CX43 endocytosis (Fykerud et al., 2012; Girao et al., 2009), no change in

CX43 half-life was associated with alterations in the levels of either of these ligases. In particular, NEDD4-mediated ubiquitylation of CX43 has been shown to increase CX43 endocytosis via an increased interaction between CX43 and EPS15, one of the adaptors in the endocytosis pathway (Girao et al., 2009). Although NEDD4-mediated ubiquitylation of CX43 has been reported, this ubiquitylation event did not result in any changes in total CX43 protein (Girao et al., 2009), suggesting a role of multiple E3 ligases in the regulation of CX43. A recent study by Fykerud et al, indicated that SMURF2, an E3 ligase closely related to NEDD4, also plays an important role in CX43 endocytosis (Fykerud et al., 2012). Although the study revealed stabilization of membrane-associated CX43 following siRNA knockdown of SMURF2, ubiquitylation of CX43 persisted even after loss of functional SMURF2 (Fykerud et al., 2012) suggesting a potential role for other E3 ligases in targeting CX43. Based on these observations, we posit that WWP1-mediated ubiquitylation is involved in CX43 turnover.

Studies described in Chapter 2 demonstrate that WWP1 polyubiquitylates CX43 (Fig. 2.5). Defining the molecular pathways and mechanisms involved in WWP1-mediated ubiquitylation of CX43 and its effect on CX43 protein stability and GJIC would contribute to understanding how GJs are regulated. Here we report that overexpression of WWP1 in HeLa-CX43 cells is associated with a decrease in CX43 half-life from two hours to less than one hour as well as a reduction in GJIC, and this effect is dependent upon the ubiquitin ligase activity of WWP1. Furthermore, *WWP1* siRNA-mediated knockdown of endogenous WWP1 in HeLa-CX43 cells resulted in increased levels (60%) of CX43 protein. Collectively, in this study we identified WWP1 as a novel

regulator of CX43 GJs that acts to modulate the level of functional CX43 at the plasma membrane available for GJIC.

## 3.2. MATERIALS AND METHODS

### Cells and plasmids

HEK 293T cells and HeLa-CX43 cells were maintained in culture in DMEM supplemented with 10% FBS plus 1% penicillin/streptomycin at 37°C with 5% $CO_2$. Transfections were performed using JetPRIME (polyPLUS) or Lipofectamine 2000 reagent (Invitrogen) according to the manufacturer's instructions. An ON-TARGET plus Human *WWP1* siRNA-SMART pool composed of four *WWP1* targeting siRNAs (target sequence 1: CCAAGAUGGAUUGAAGAGUU; target sequence 2: GAAAAGCAACGAUAGAUUU; target sequence 3: GAACGCGGCUUUAGGUGGA; target sequence 4: GGUCUGAUACUAGUAAUAA) and a non-targeting pool (D-001810-10-05) were purchased from Thermoscientific. 25 ng of siRNA was used to transfected cells using HiPerFect transfection reagent (Qiagen, 301704)

### Western blot analysis

Cells were harvested using Triton X-100 lysis buffer (150 mM NaCl; 50 mM Tris-HCl, pH 7.5; 0.5% Triton X-100 supplemented with cocktail protease inhibitors plus EDTA, 2 mM sodium orthovanadate, and 10 mM iodoacetamide). 50 µg of protein was loaded and separated on a gradient 4-15% TGX-SDS gel (Bio-Rad), and transferred to PVDF membrane (Bio-Rad). A blocking buffer (5% non-fat dry milk in TBST) was used to block non-specific binding of the primary antibodies to the membrane. The blot was probed using one of the following primary antibodies for 16 hours at 4°C: anti-CX43

(Sigma, C6219), anti-Myc (Santa Cruz, 9E10), anti-tubulin (Sigma, T5168), and anti-WWP1 (Abnova, clone 1A7) followed by probing with the corresponding HRP-tagged secondary antibodies. Signals were visualized using ECL reagent (Millipore, Immobilon Western) and images were acquired using the FluorChem E Western blot imaging system (Protein Simple) and images were analyzed using AlphaView software.

**Cyclohexamide chase assay**

HeLa-CX43 cells transfected either with Myc-WWP1 or with Myc-C886S were treated with 100 ng/mL PMA for 1 hour followed by treatment with 100 µg/mL cyclohexamide (CHX). Cells were harvested using RIPA (Radio immunoprecipitation assay) buffer (150mM NaCl, 50mM Tris-HCl, 1% NP-40, 0.5% sodium deoxycholate, 0.1% SDS (sodium dodecylsulphate) at 0, 1, 2, 3, and 4 hours post CHX treatment. Western blots were performed using the indicated primary antibodies as described above. The relative remaining level of CX43 was calculated by first normalizing the level of CX43 protein for each sample using the tubulin loading control. Subsequently a ratio of normalized CX43 after CHX addition to normalized CX43 before cyclohexamide addition was calculated for each of the four indicated time points. The experiment was repeated three times and error bars were calculated from triplicates. The half-life of the CX43 protein is estimated to be the time point after the addition CHX at which the CX43 protein level is 50% of the CX43 at time zero.

**Triton X-100 solubility assay**

293T cells were harvested using triton X-100 lysis buffer (150 mM NaCl; 50 mM Tris-HCl, pH 7.5; 0.5% Triton X-100 supplemented with cocktail protease inhibitors plus EDTA, 2 mM sodium orthovanadate, and 10 mM iodoacetamide). Cell lysates were centrifuged at 22,000 x g for 30 min at 4°C. The Triton X-100 insoluble pellet was re-suspended in Triton X-100 lysis buffer plus 0.5% SDS and sonicated three times at 50% amplitude for 5 seconds. Triton X-100 soluble and insoluble fractions were run on gradient 4-15% TGX SDS polyacrylamide gel and transferred to a PVDF membrane. Western blots for CX43 were performed as indicated above. Alpha View imaging software was used to quantify band intensities and GraphPad Prism software was used to perform statistical analysis and draw graphs. The experiments were repeated twice and the values are presented as the mean and SEM of duplicates.

**Scrape loading assay**

HeLa-CX43 cells plated on coverslips were transfected with either mCherry-WWP1 or mCherry-C886S. Forty eight hours post transfection, confluent cells were rinsed with 1X PBS, scraped using a sharp razor blade and then incubated with 0.25% Lucifer yellow dye for 4 min at room temperature. Cells were subsequently rinsed three times with 1X PBS followed by fixation with 4% paraformaldehyde (PFA) for 15 min. Between twenty to thirty images along the scratch were acquired with 20X objective of an Axio Vision Zeiss wide field epifluorescent microscope using Zeiss Axiocam MRM5 camera. For every image, the distance between the center of the scratch and the farthest cell that has taken up the dye was measured and reported in arbitrary units (AU). All

measurements were calculated using ImageJ software (NIH) and graph plotting and statistical analysis was performed using GraphPad Prism.

## 3.3. RESULTS

### WWP1 induces increased CX43 turnover

To further understand the role of WWP1-mediated ubiquitylation on CX43 protein stability described in Chapter 2, we measured the half-life of CX43 in HeLa-CX43 cells using a CHX chase assay. In this assay, HeLa-CX43 cells transfected with either Myc-WWP1 or Myc-C886S were first stimulated with 100 ng/mL PMA for 1 hour and subsequently treated with 100 µg/mL of CHX for 1, 2, 3, or 4 hours. Cells were harvested, lysed, and a ratio of the amount of CX43 protein after CHX treatment to the level of CX43 before CHX treatment (0 hour) was calculated for each time point. All protein measures were standardized to a tubulin loading control. This experiment was done in triplicates to obtain averages and standard deviations for each time point and graphed as a line graph to approximate half-life (Fig. 3.1). This analysis indicated that overexpression of WWP1 resulted in increased CX43 turnover with a reduction in CX43 half-life from two hours to fifty minutes compared to Myc-C886S transfected or untransfected cells (Fig. 3.1). Thus, the ubiquitylation of CX43 by WWP1 resulted in increased turnover of this GJ protein.

We further investigated the role of WWP1 overexpression on the levels of GJ incorporated versus cytoplasmic CX43 in 293T cells by co-transfecting them with CX43 and either Myc-WWP1 or Myc-C886S after PMA stimulation for 1hour. CX43 in the GJ plaque is insoluble in triton X-100 lysis buffer and migrates more slowly upon

electrophoresis (Sirnes et al., 2008), hence a triton X-100 solubility assay was used to differentiate between plasma membrane (junctional) and cytoplasmic (non-junctional) CX43. Western blot analysis of the junctional and non-junctional fractions of CX43 showed that WWP1 overexpression leads to a dramatic decrease in both junctional and non-junctional CX43 protein (90% and 75%, respectively) levels compared to cells transfected with the ligase-dead version of WWP1 (C886S, Fig. 3.2). These data indicate that overexpression of WWP1 does not preferentially affect a subset of the intracellular pools of CX43; rather, its effect is globally evidenced.

**Overexpression of WWP1 leads to down regulation of GJIC**

Since it appeared that the levels of CX43 at the plasma membrane were regulated by the ubiquitin ligase activity of WWP1, we hypothesized that GJIC would be altered with changing levels of WWP1. GJIC function is traditionally measured by a scrape loading or dye transfer assay which measures the passage of small tracer dyes such as Lucifer yellow through gap junctions. Lucifer yellow is impermeable through the plasma membrane and is introduced to cells through injection or scraping. Once introduced into the cell the dye travels between adjacent cells through GJ channels and the rate of dye migration is used as a measure of GJ function. A scrape loading assay was performed on a confluent layer of non-stimulated HeLa-CX43 cells overexpressing either mCherry-WWP1 or mCherry-C886S and the lucifer yellow mobility was compared to that in untransfected HeLa-Cx43 cells. The furthest distance traveled by the dye from the middle of the scratch was determined for each culture condition in twenty to thirty 20X magnification fields using ImageJ imaging software (NIH). Values are presented as means and SEM and one-way ANOVA with Bartlett's correction was performed to test

statistical significance. This analysis demonstrated a statistically significant reduction (36%) in dye transfer through the GJ channels in those cells overexpressing wild type WWP1 as compared to HeLa-CX43 cells transfected with mCherry-C886S or untransfected cells ($p<0.001$) (Fig. 3.3). Further, these functional changes appear to be dependent upon the ubiquitin ligase activity of WWP1 as the C886S ligase-dead mutant had no detectable effect on GJIC and suggests that dosage of WWP1 may influence GJIC.

**Depletion of endogenous WWP1 leads to CX43 protein stabilization**

To assess the physiological role of WWP1 on CX43 turnover, endogenous WWP1 was depleted in HeLa-CX43 cells using a targeting siRNA pool. 48 hours post transfection, cells were treated with 100mg/mL PMA for one hour, and the level of CX43 was subsequently assessed by harvesting cells using Laemmli sample buffer. Western blot analysis of triplicates showed that loss of functional WWP1 using the targeting siRNA pool yielded a 60% increase in total CX43 compared to similarly treated cells that were either untransfected or transfected with a non-targeting siRNA pool (Fig. 3.4A). These data confirm that the decrease in CX43 observed after WWP1 overexpression is not an artifact but that WWP1 has a physiological role in regulating CX43.

To determine whether loss of WWP1 function affected the entire pool of CX43 or a particular subcellular fraction, a triton X-100 solubility assay was performed in HeLa-CX43 cells transfected with either WWP1 targeting siRNA pool or non-targeting siRNA pool. Forty eight hours post transfection, cells were treated with 100ng/ml PMA for one hour and cells were harvested using Triton X-100 lysis buffer followed by high speed centrifugation to fractionate triton X-100 soluble and insoluble CX43.The experiment

was performed in triplicates and the level of CX43 was quantified using AlphaView imaging software. GraphPad statistical analysis software was used to calculate one way ANOVA. Immunoblot analysis of triton X-100 soluble and insoluble fractions of CX43 showed increased levels of junctional CX43 on the membrane. However, the level of cytoplasmic or non-junctional CX43 was decreased which might be a consequence of increased CX43 recycling to the plasma membrane or lack of CX43 internalization (Fig. 3.4B).

## 3.4. DISCUSSION

Here we demonstrate for the first time that the E3 ubiquitin ligase WWP1 regulates CX43 stability and GJIC. This regulation was physiologically relevant as opposite effects were observed with overexpression of WWP1 versus knockdown of the endogenous ligase in two distinct cell lines. Further, the ubiquitin ligase activity of WWP1 was necessary for these effects as overexpression of a ligase-dead version of WWP1 showed no change relative to untransfected cells. Although previous studies have identified NEDD4 and SMURF2 as regulators of CX43 endocytosis (Fykerud et al., 2012; Girao et al., 2009) none of the studies have shown changes in CX43 half-life. In particular, NEDD4-mediated ubiquitylation of CX43 has been shown to increase CX43 endocytosis via an increased interaction between CX43 and EPS15, one of the adaptors in the endocytosis pathway (Girao et al., 2009). A recent study by Fykerud et al, indicated that SMURF2, an E3 ligase closely related to NEDD4, also plays an important role in CX43 endocytosis (Fykerud et al., 2012). Although the study revealed stabilization of membrane-associated CX43 following siRNA knockdown of SMURF2, ubiquitylation of CX43 persisted even after loss of SMURF2 (Fykerud et al., 2012). Based on these

observations, we suggest that WWP1-mediated ubiquitylation is involved in CX43 turnover and in this study we aimed to get a better understanding of the role of WWP1 on CX43 GJ level and function. Subsequent half-life measures in HeLa-CX43 cells revealed that overexpression of only catalytically WWP1 resulted in increased CX43 turnover.

To further understand the role of WWP1 ubiquitylation on gap junction function, a scrape loading or dye transfer assay was performed on HeLa-CX43 cells. Previous studies have reported a transient decrease in GJIC upon treatment of cells in culture with PMA. To delineate the role of PMA induced phosphorylation and WWP1 induced ubiquitylation on GJIC, the scrape loading assay was conducted in the absence of PMA. The fact that GJIC was reduced upon WWP1 overexpression even in the absence of PMA suggests that WWP1 might be playing a role in maintaining the physiological CX43 level. Our data indicated that WWP1 overexpression caused a significant reduction on dye transfer through gap junction channels. This reduction in GJIC was not seen when the ligase dead mutant was utilized. Collectively, our data indicate a novel role of WWP1 on the CX43 stability and GJIC.

In this study, the role of endogenous WWP1 on CX43 regulation and GJ function was assessed through siRNA-mediated knockdown of WWP1 in PMA-stimulated HeLa-CX43 cells. Loss of WWP1 expression was associated with a 60% increase in total CX43 protein as compared to similarly treated cells transfected with a non-targeting siRNA pool or to untransfected cells that were PMA-stimulated. Additionally, a Triton X-100 solubility assay was conducted HeLa-Cx43 cells to determine if the increased CX43 is due to stabilization of membrane or cytoplasmic fractions of CX43. Our data indicated that WWP1 knockdown is associated with increased junctional (membrane) and

reduced cytoplasmic CX43 levels. This observation is similar to previous reports on siRNA knockdown of SMURF 2 and NEDD4 that showed an increased level of CX43 on the plasma membrane. The reduction in non-junctional (cytoplasmic) CX43 after loss of WWP1 could be explained either by decreased endocytosis of CX43 or by increased recycling of CX43 to the plasma membrane. It is tempting to speculate that the latter is the cause for the effects seen upon knockdown of WWP1 since a previous study alludes to the existence of a CX43 recycling pathway (Boassa et al., 2010). Complementary to this observation are the results obtained from performing the triton X-100 solubility in PMA-stimulated 293T cells after WWP1 overexpression. With increased expression of WWP1, both junctional (non-soluble) and non-junctional (soluble) levels of CX43 were significantly decreased by ninety and seventy five percent, respectively. However, the decreased junctional CX43 level upon WWP1 could be explained by the degradation of the pool of CX43 in the cytoplasm since proteasomal and lysosomal inhibitors were not utilized in these assays. To determine the molecular mechanisms of CX43 turnover, intracellular trafficking studies on the level of CX43 in different endocytic compartments will be required and we have addressed the same question in the next chapter.

### 3.5. FIGURES

A

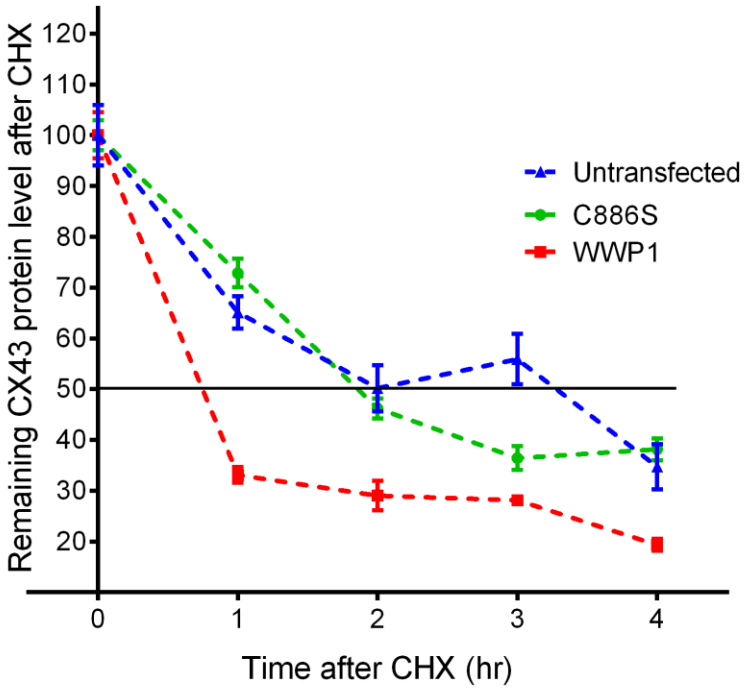


B

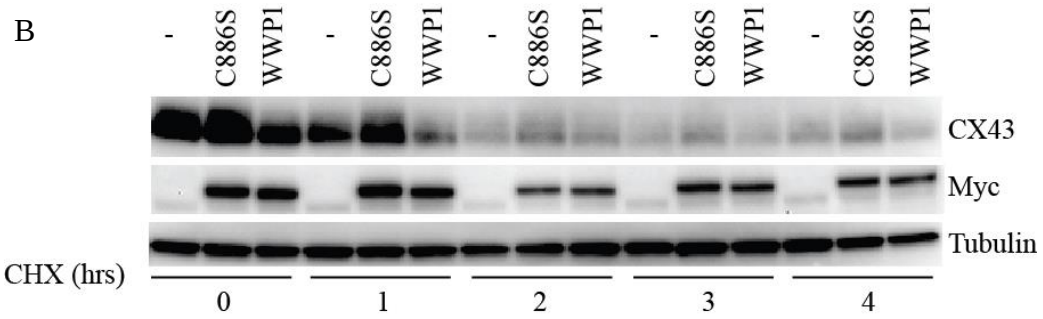

Figure 3.1 WWP1 overexpression increases CX43 turnover. A. HeLa-CX43 cells transfected either with Myc-WWP1 or Myc-C886S were treated with 100 ng/mL PMA followed by 100 µg/mL of cyclohexamide (CHX) for 1, 2, 3, and 4 hours at which time the level of CX43 protein was assessed. Tubulin was used as a loading control and the remaining CX43 after CHX addition was standardized against CX43 before CHX addition at time 0. The values are presented as means and SEM of triplicates. The half life of CX43 is the time at which 50% of the CX43 protein is measured as compared to Cx43 levels before the introduction of CHX. B. The experiment was conducted in triplicates and a representative western blot showing CX43 protein level is shown here.

A

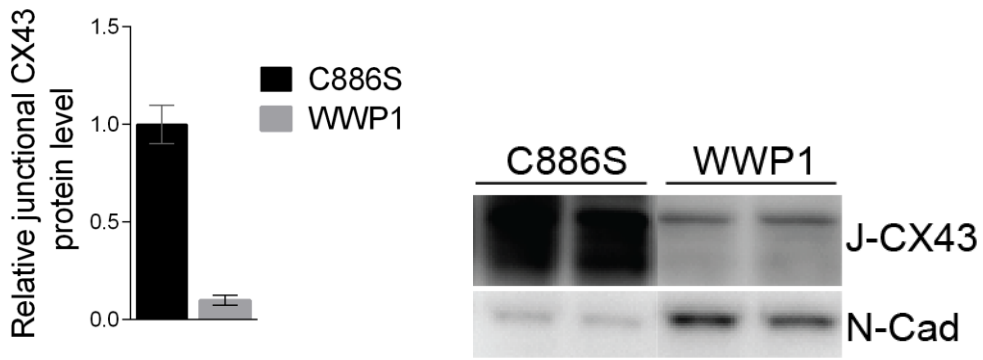


B

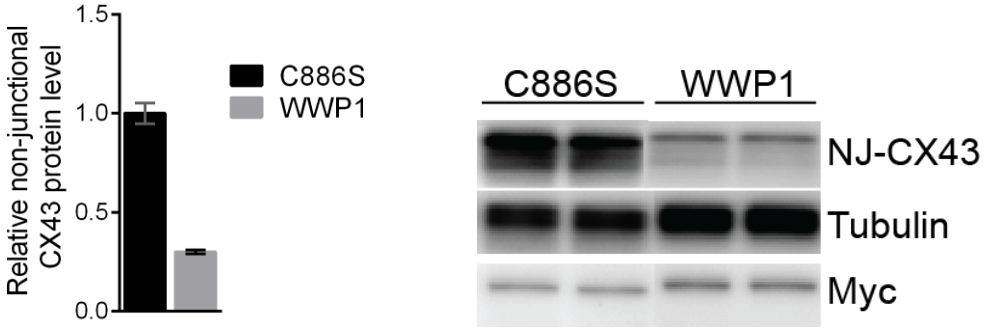


Figure 3.2 WWP1 overexpression reduces junctional and non-junctional cellular pools of CX43. 293T cells were co-transfected with CX43 and either Myc-WWP1 or Myc-C886S. 48 hours post-transfection cells were treated with 100ng/ml PMA for 1 hour and cellswere harvested using Triton X-100 lysis buffer. A. A bar graph showing Cx43 levels relative to mutant C886S transfected cells. WWP1 overexpression leads to a 90% reduction in Triton X-100 insoluble junctional CX43 compared to mutant WWP1 (C886S). Values are presnted as means and SEM of duplicates. A student's t-test was used to determine significance analysis (p=0054). B. WWP1 over expression leads to decreased (75%) non-junctional/cytoplasmic CX43 proetein level compared to C886S. The experiment was conducted in duplicates and Student's t-test analysis with Welch's correction showed a significant reduction in CX43 protein upon overexpression of WWP1.($p<0.05$).

A

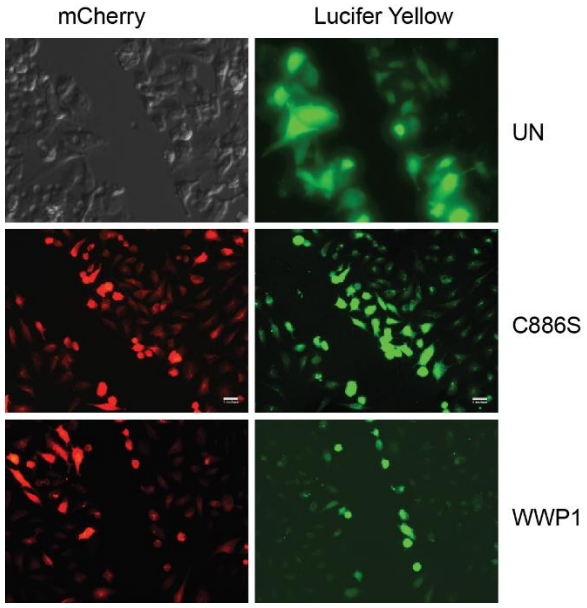


B

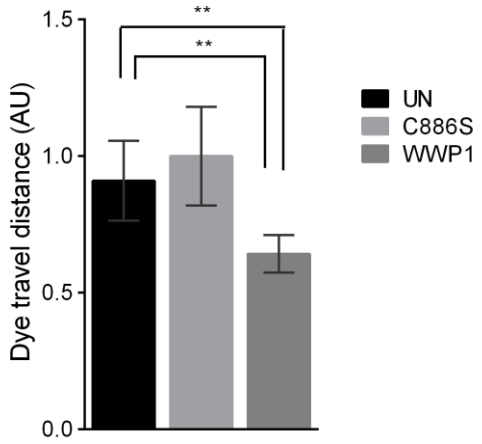


Figure 3. 3 Over expression of WWP1 leads to down regulation of GJIC. A scrape loading assay was performed on unstimulated HeLa-CX43 cells transfected with either mCherry-WWP1 or mCherry-C886S as well as on untransfected control cells (UN). Cells were injured by scraping followed by the addition of 0.25% Lucifer yellow for 4 min. B. The farthest dye migration was measured in arbitrary units from the center of the scratch using ImageJ (NIH) software. A bar graph showing the means and SEM (n=30) of dye migration in AU. Cells transfected with WWP1 had a statistically significant decrease (36%) in dye transfer between adjacent cells as compared to C886S-transfected or untreated cells, ($p<0.001$) indicating that the ubiquitin ligase activity of WWP1 was required to down regulate GJIC.

A

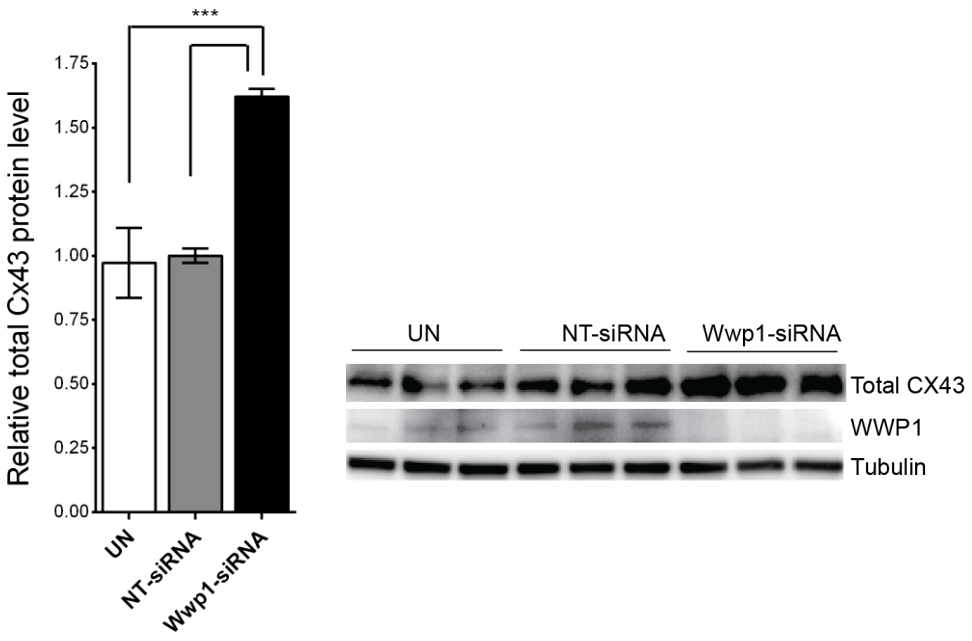
***
Relative total Cx43 protein level
1.75
1.50
1.25
1.00
0.75
0.50
0.25
0.00
UN
NT-siRNA
Wwp1-siRNA
UN
NT-siRNA
Wwp1-siRNA
Total CX43
WWP1
Tubulin

B

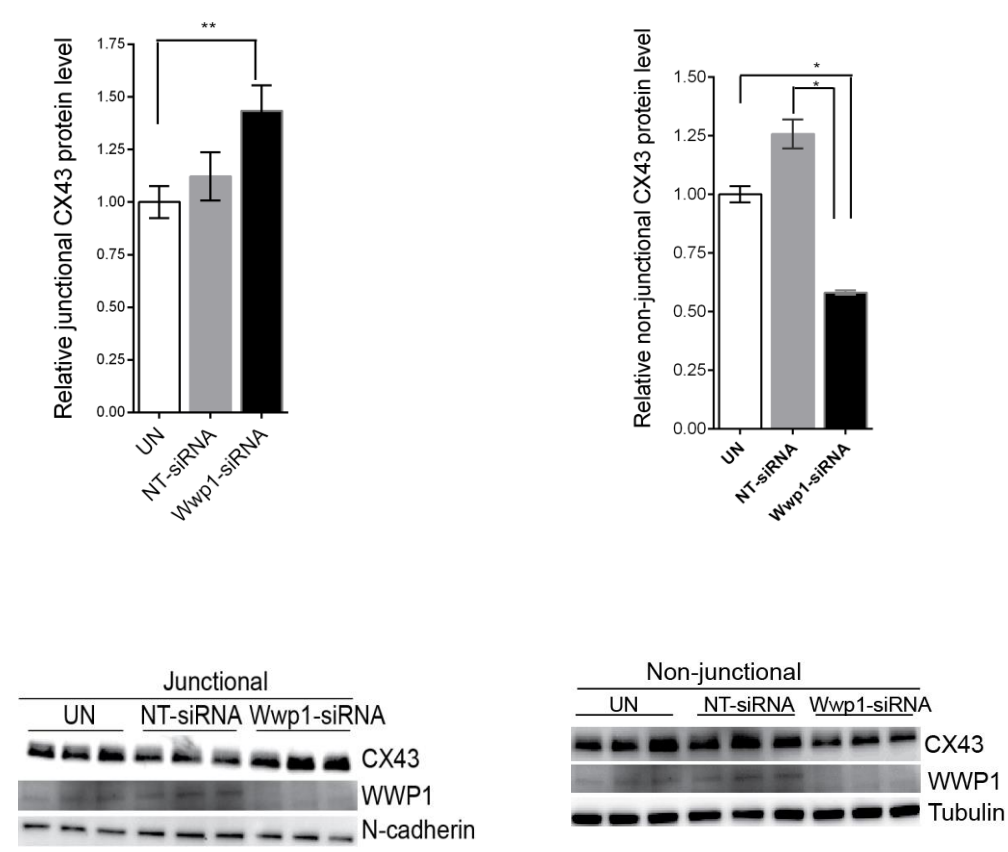
**
Relative junctional CX43 protein level
1.75
1.50
1.25
1.00
0.75
0.50
0.25
0.00
UN
NT-siRNA
Wwp1-siRNA
*
*
Relative non-junctional CX43 protein level
1.50
1.25
1.00
0.75
0.50
0.25
0.00
UN
NT-siRNA
Wwp1-siRNA
Junctional
UN
NT-siRNA
Wwp1-siRNA
CX43
WWP1
N-cadherin
Non-junctional
UN
NT-siRNA
Wwp1-siRNA
CX43
WWP1
Tubulin

Figure 3.4 Loss of function of endogenous WWP1 results in stabilization of cell membrane CX43. A. HeLa-CX43 cells were transfected with WWP1-siRNA or non-targeting siRNA (NT-siRNA). 48 hours later cells were treated with 100 ng/mL PMA for 1 hour and then harvested using Laemelli sample buffer and total CX43 was quantified and standardized using tubulin as a loading control and the CX43 protein relative to NT-siRNA was calculated.The experiments were conducted in triplicates and quantification of protein leveles was done using AlphaView software. Knockdown of WWP1 is associated with a 60% increase in total CX43 level as compared to untransfected (UN) or NT-siRNA transfected. Values are presnted as means and SEM of triplicates. One-way ANOVA was used to test for significance (n=3), ($p<0.005$). B. HeLa-Cx43 cells were transfected with WWP1-siRNA pool or NT-siRNA pool. Cells were treated with 100ng/ml PMA for 1 hour and were harvested using Triton X-100 lysis buffer followed by Triton X-100 solubulity assay to fractionate GJ plaque associated insoluble CX43 versus cytoplasmic/soluble CX43. ). Loss of WWP1 was associated with a significant increase in junctional (plasma membrane) CX43 and a decrease in the non-junctional (cytoplasmic) fraction of CX43. One-way ANOVA was perforemed to assess statitical significance (n=3), ($p<0.05$).

# CHAPTER FOUR

## WWP1-Mediated Ubiquitylation Targets CX43 for Lysosomal Degradation

## 4.1. INTRODUCTION

GJs are dynamic plasma membrane structures that undergo constant turnover. GJ internalization is reported to involve the CME machinery (Falk et al., 2012; Gumpert et al., 2008; Piehl et al., 2007). The CME pathway involves a complex of proteins including clathrin and the clathrin adaptors AP2, DAP2, DYNAMIN2, MYOSIN VI, and actin (Kirchhausen et al., 2014). During GJ endocytosis, both membranes forming the channel are endocytosed into one of the cells joined by the GJs to form a double membrane vesicle termed annular junction or connexesome (Piehl et al., 2007). Annular junctions are further processed into single membrane vesicles that will eventually fuse with the early endosome (Jordan et al., 2001). Ubiquitylation serves as an important signal for internalization and endocytic sorting of membrane proteins. Endocytic adaptors such as EPS15 and EPSIN have UIM and a clathrin binding domain that link ubiquitin tagged cargo to clathrin-coated pits during CME (Kirchhausen et al., 2014).

Early endosomes serve as vesicular sorting stations in the endocytotic pathway with subdomains that promote trafficking of cargo towards the lysosome for degradation or to other regions that facilitate recycling of integral membrane proteins back to the plasma membrane (Raiborg and Stenmark, 2009). Sorting in the early endosomes is achieved by adaptor proteins on the endosomal membranes. One class of well characterized adaptors are the Rab GTPases, RAB4 and RAB5 (Henne et al., 2011; Luzio et al., 2009). The RABs recruit endosomal sorting complex for transport (ESCRT) complex proteins, which are involved in cargo sorting to various intracellular destinations (Henne et al., 2011). The ESCRT machinery consists of four complexes, ESCRT-0, I, II and III and performs three distinct but connected functions: first, it recognizes

ubiquitylated cargo and prevents recycling and retrograde trafficking of the cargo; second, it deforms the endosomal membrane allowing cargo to be sorted into endosomal invaginations; third, it catalyzes the final abscission of the endosomal invaginations, forming the intraluminal vesicles (ILVs) that contain the sorted cargo (Raiborg and Stenmark, 2009; Nikko and Andre, 2007).

Components of the ESCRT complex have multiple ubiquitin binding domains that enable ubiquitin-dependent sorting of target proteins through selective binding of ubiquitylated cargo. The ESCRT-0 complex consists of the subunits HRS and STAM and is considered to be a filter that retains ubiquitylated cargo on the endosomal membrane (Luzio et al., 2009; Piper and Luzio, 2007). The HRS subunit has the ability to bind the endosomal lipid phosphatidylinositol-3-phosphate thereby nucleating the assembly of the ESCRT-0 complex at endosomal membranes. The UIMs in ESCRT-0 have low affinity for ubiquitin raising the question as to how this complex can function in efficient sorting of ubiquitylated cargo. One possibility is that these UIMs have the ability to bind multiple ubiquitins, thereby strengthening the overall interaction. For instance, the well characterized membrane receptor, EGFR, has been reported to be ubiquitylated at multiple residues and its multi-mono-ubiquitylation favors EGFR binding to HRS (Huang et al., 2006; Umebayashi et al., 2008). In addition, the multi-mono-ubiquitylation of EGFR has been reported to occur within multiple subcellular domains, including at the plasma membrane as well as at in the early endosome after its internalization, supporting the idea that multiple E3 ligases can act on a single substrate to possibly increasing substrate affinity for UIMs (Eden et al., 2012).

Besides substrate binding, HRS is also responsible for recruiting the ESCRT-I complex to early endosomes via its binding to the TSG101 subunit of ESCRT-1 (Luzio et al., 2009; Raiborg and Stenmark, 2009). Vps28, another subunit of ESCRT-I, binds to Vps36, a component of ESCRT-II in order to recruit the ESCRT-II complex (Raiborg and Stenmark, 2009). Once both ESCRT-I and ESCRT-II are assembled at the early endosome, membrane deformation is initiated and subdomains of the plasma membrane bud into the lumen of the early endosomes to form ILVs. Early endosomes with ILVs will mature into MVBs or late endosomes and fuse with the lysosomes for their contents to be degraded by lysosomal enzymes (Pryor and Luzio, 2009; Raiborg and Stenmark, 2009). The ESCRT-III complex is involved in the transition from ILVs to MVBs by mediating membrane scission and recruitment of deubuquitylating enzymes (DUBs) (Wright et al., 2011). DUBs catalyze the removal of ubiquitin from a substrate and mediate the recycling of ubiquitin, thereby avoiding depletion of the cellular ubiquitin pool (Raiborg and Stenmark, 2009; Wright et al., 2011). Thus, by deubiquitylating cargo and diverting its passage away from the lysosome, DUBs act as antagonists to the E3 ligases that promote cargo internalization towards the lumen of the early endosomes.

Several lines of evidence indicate a role for ubiquitylation in the internalization of CX43 (Leithe and Rivedal, 2004d; Leithe and Rivedal, 2004b). In particular, it has been shown that ubiquitin is recruited to GJs in response to PMA treatment (Leithe and Rivedal, 2004a). Ubiquitylation of CX43 is essential for its recognition by the UIMs of endocytic adaptor proteins like EPS15 at the plasma membrane, as EPS15-mediated endocytosis of CX43 was enhanced when CX43 was ubiquitylated by NEDD4 (Girao et al., 2009). In contrast, depletion of *EPS15* with siRNAs led to the accumulation of CX43

on the plasma membrane and an increase in the size of GJ plaques (Girao et al., 2009). Although these studies demonstrated the importance of NEDD4-mediated ubiquitylation on CX43 endocytosis, no change in total CX43 protein was detected. It is tempting to speculate that additional ubiquitylation events occur in the early endosome to increase binding affinity of HRS for CX43, thus promoting trafficking of CX43 to the lysosome for degradation. CX43 has been shown to interact with components of the ESCRT machinery such as HRS. In particular, depletion of the ESCRT complex proteins *HRS* and *TSG101* using siRNA yields an accumulation of ubiquitylated CX43 in early endosomes as well as enlargement of early endosomes (Leithe et al., 2009). In the case of CX43, the ligase responsible for these additional modifications has not been identified.

As is indicated in chapter 3 as well as in the mouse model described in chapter 2, increased expression of WWP1 results in decreased CX43 half-life. Further, as shown in Chapter 2, WWP1 mediates K27- and K29-linked polyubiquitylation of CX43. The type of ubiquitylation determines the fate of a substrate, but the role of atypical polyubiquitin chains such as K27- and K29-linked chains is not well documented, although there has been some association of K29 linkages with lysosomal degradation (Chastagner et al., 2006). In an effort to understand the role of WWP1-mediated ubiquitylation on CX43 trafficking, we utilized immunofluorescence to analyze the co-localization of CX43 and markers of post-endocytic compartments including early, late, and recycling endosomes in response to overexpression or knockdown of WWP1. Our data demonstrate that the ligase activity of WWP1 promotes trafficking of CX43 from the early endosome to the late endosome while loss of function of WWP1 is associated with increased recycling of CX43. Lysosomal inhibition prevented the degradation of CX43 even when WWP1 was

overexpressed. Taken together, these data place the activity of WWP1 squarely and prominently in the center of the intracellular CX43 sorting pathway.

## 4.2. MATERIALS AND METHODS

### Tissue culture and reagents

Human cervical carcinoma (HeLa) cells stably transfected with CX43 (HeLa-CX43) and Human Embryonic Kidney (HEK) 293T cells were maintained in culture in 10% complete media (DMEM, 10% FBS, 1% penicillin/streptomycin) at 37°C with 5% $CO_2$. Transfections were performed using JetPRIME (PolyPLUS) and Lipofectamine-2000 reagent (Invitrogen) according to the manufacturer's instructions. PMA (P81391), Dynasore (D7693), and anti-CX43 antibody (C6219) were purchased from Sigma. Anti-EEA1 (BD Scientific, 610456) anti-CD63 (Developmental Studies Hybridoma Bank, H5C6), and anti-RAB11 (Cell Signaling, 3539) antibodies were used to stain the early, late and recycling endosomes, respectively. ON-TARGET plus Human WWP1 siRNA-SMART pool composed of four *WWP1* targeting siRNAs (target sequence 1: CCAAGAUGGAUUGAAGAGUU; target sequenct 2: GAAAAGCAACGAUAGAUUU; target sequence 3: GAACGCGGCUUUAGGUGGA; target sequence 4: GGUCUGAUACUAGUAAUAA) and a non-targeting pool (D-001810-10-05) were purchased from Thermoscientific. 25 ng of siRNA was used to transfected cells using HiPerFect transfection reagent (Qiagen, 301704).

**Immunofluorescence staining**

HeLa-CX43 cells grown on coverslips were transfected using either mCherry-WWP1 or mCherry-C886S plasmids. Forty-eight hours following transfection, cells were treated with 100 ng/mL PMA for one hour. Cells were rinsed with PBS and fixed in 4% PFA for 15 min at room temperature, rinsed 3X with PBS followed by blocking using a blocking buffer (5% normal goat serum, 1% BSA and 0.3% Triton X-100 in PBS) for 1 hour at room temperature. Cells were stained using primary antibodies overnight at 4°C followed by incubation with fluorophore-conjugated $F(ab')_2$ fragment secondary antibodies (Jackson Immunoresearch). Cover slips were mounted using Fluoro-Gel mounting media (Electron Microscopy Sciences). Images were acquired using the following microscopes: 100X objectives of Leica DMI6000B microscope (Hamamatsu Camera C10600); 63X objectives of Zeiss AxioImager A1 microscope (Zeiss Axiocam MRM5 camera), and Olympus IX81 (Hamamatsu C10600 camera). 2D deconvolution was performed using MetaMorph Basic for some of the images to remove out of focus light.

**Co-localization and statistical analysis**

Between twenty five to thirty five transfected with mCherry-WWP1 or mCherry-C886S (only cells with red fluorescent intensities ranging between thirty three to seventy five pixels were selected in order to analyze transfected cells with similar levels of expression) and untransfected cells were used for Pearson's co-localization coefficient analysis. The NIH ImageJ co-localization threshold plugin (Schneider et al., 2012) software was used to calculate co-localization coefficients. The co-localization co-efficient values range between 1 to -1 where 1 indicates perfect positive localization, 0

means no co-localization and -1 total negative co-localization. The transfections were performed at least three times in order to get the required number of cells. GraphPad Prism was used to perform Student's t-test and ANOVA statistical significance analysis and to make graphs.

**Protein extraction and Western blot analysis**

HEK293T and HeLa-CX43 cells were rinsed with ice cold PBS and then lysed using Triton X-100 lysis buffer (150 mM NaCl, 50 mM Tris-HCl pH 7.5, 0.05% Triton X-100 plus a protease inhibitor cocktail; 10 mM orthovanadate and 2 mM sodium iodoacetamide). The cell extracts were denatured by boiling in 2X Laemmli sample buffer for 5 min followed by electrophoresis on a denaturing 4-15% gradient polyacrylamide gel and then transferred to a PVDF membrane. Membrane blocking was performed using 5% nonfat dry milk in TBST followed by incubation with the corresponding primary and secondary antibodies. Protein levels were quantified as band intensities using Alpha View imaging software. Experiments were repeated at least three times and the average of the triplicates was used to calculate averages and standard deviation calculations.

**Triton X-100 solubility assay**

293T cells were harvested using Triton X-100 lysis buffer (150 mM NaCl; 50 mM Tris-HCl, pH 7.5; 0.5% Triton X-100 supplemented with cocktail protease inhibitors plus EDTA, 2 mM sodium orthovanadate, and 10 mM iodoacetamide). Cell lysates were centrifuged at 22,000 x g for 30 min at 4°C. The insoluble pellet was re-suspended in Triton X-100 lysis buffer plus 0.5% SDS and sonicated twice at 50% amplitude for 5

seconds. Triton X-100 soluble and insoluble fractions were separated on 4-15% gradient polyacrylamide gels (TGX, Bio-Rad). Experiments were performed in duplicates.

## 4.3. RESULTS

### PMA promotes internalization of CX43 to the early endosome

To study the role of WWP1 in the intracellular trafficking of CX43 from the endosome to the lysosome, we first sought to establish an experimental system. In particular, we wanted to promote the internalization of CX43. Therefore, we treated HeLa-CX43 cells with PMA. In agreement with previously published studies (Falk et al., 2012; Leithe and Rivedal, 2004d; Sirnes et al., 2008), PMA treatment changed the localization pattern of CX43 from being predominantly at the cell surface to being intracellular with a punctate pattern (Fig. 4.1A). To verify that this treatment was promoting trafficking of CX43 through the endocytic pathway, PMA-treated HeLa-CX43 were immunofluorescently labelled with antibodies recognizing CX43 and the early endosome marker EEA1. Co-localization analysis showed that a subset of the CX43 pool did indeed localize to the early endosome (yellow in Fig. 4.1A) and that this interaction was maximal after one hour of PMA treatment (Fig. 4.1B). Therefore, we utilized this time point for subsequent analysis.

Further confirmation of the endocytosis-promoting effect of PMA was obtained in the HEK293T cell line using a Triton X-100 solubility assay. Since only the CX43 incorporated into the GJ plaque is insoluble in Triton X-100 lysis buffer, this assay can discriminate between junctional CX43 and cytoplasmic pools. Therefore, increased endocytosis of CX43 should correlate with increased Triton X-100 solubility. Indeed, our

data showed that exposure of CX43-transfected HEK293T cells to PMA decreases the level of membrane CX43 while increasing cytoplasmic CX43 (Fig. 4.1C). Further, addition of the CME inhibitor dynosore reversed this effect, highlighting the fact that PMA-induced CX43 endocytosis is mediated by the CME pathway (Fig. 4.1D).

**WWP1 promotes trafficking of CX43 from the early endosome to the lysosome**

To examine the role of WWP1-mediated ubiquitylation on CX43 trafficking, HeLa-CX43 cells were transfected with either mCherry-WWP1 or mCherry-C886S, treated with PMA, and then immunofluorescently labelled using anti-CX43 and anti-EEA1 antibodies. Between 25 -35 transfected cells (defined as cells with red fluorescence intensities between 33-75 pixels) were selected and co-localization analysis was measured as Pearson's coefficient of co-localization using the threshold co-localization plugin of ImageJ software. These values were averaged and used to calculate mean and standard deviations. One-way ANOVA was used to test statistical significance. Our data showed no significant difference in the co-localization of CX43 and EEA1 among wild type and mutant WWP1 transfected or untransfected cells (Fig. 4.2A &B). This indicates that PMA alone is sufficient to mediate the internalization of CX43 from the plasma membrane to the early endosome as the ubiquitin ligase activity of WWP1 does not significantly alter this process. However, immunofluorescent staining of PMA-treated HeLa-CX43 cells transfected with mCherry-WWP1 or mCherry-C886S did show increased co-localization of CX43 with the late endosomal marker CD63 upon expression of wild type WWP1 compared to either mutant WWP1 transfected or to untransfected cells (Fig. 4.3 A & B). This indicates that trafficking of CX43 from the early endosome to the late endosome was promoted by the ubiquitin ligase activity of WWP1.

**WWP1 overexpression leads to lysosomal degradation**

Because there was increased co-localization between CX43 and the late endosomal marker CD63 when wild type WWP1 was overexpressed in HeLa-CX43 cells (Fig. 4.3 A&B) and because overexpression of WWP1 resulted in decreased levels of CX43 (Fig. 3.1 & 3.2), we hypothesized that ubiquitylation of CX43 by WWP1 promoted lysosomal degradation of CX43. To test this hypothesis, we transfected HeLa-CX43 cells with either Myc-WWP1 or with Myc-C886S. Forty-eight hours later, cells were PMA-stimulated and treated with a lysosomal inhibitor ($NH_4Cl$) for three hours. Total protein was extracted from the cells using Laemmli sample buffer and the levels of CX43 protein were measured using western blot. First the protein levels were normalized to tubulin and all were compared to the ratio of untreated CX43. Consistent with what we had observed in HEK293T cells (Fig. 3.2 A & B), overexpression of only the wild type form of WWP1 resulted in a significant decrease in CX43 protein (Fig. 4.4 A & B). However, this effect was completely abrogated upon lysosomal inhibition (Fig. 4.4 A & B).

**Loss of function of endogenous WWP1 results in decreased late endosomal trafficking of CX43**

Because our previous data were generated using overexpression, we sought to investigate the physiological role of WWP1 on CX43 trafficking by knocking down endogenous WWP1 in HeLa-CX43 cells using targeting siRNA pools and compared the localization of CX43 to when HeLa-CX43 cells were transfected with a non-targeting siRNA pool. After staining with anti-CX43 and anti-CD63 antibodies, thirty to forty cells were evaluated for the co-localization of these proteins. Pearson's co-localization

coefficient values were averaged and compared to untransfected cells. One-way ANOVA was used to test statistical significance. Our analysis revealed a statistically significant reduction in the co-localization of CX43 with CD63 in the absence of WWP1 (Fig. 4.5). This, in combination with the complementary overexpression data, supports the assertion that ubiquitylation of CX43 by WWP1 is necessary for trafficking of CX43 from the early endosome to the late endosome, although this modification plays no apparent role in the internalization of CX43.

**Loss of function of endogenous WWP1 results in increased recycling of CX43**

Because there was less trafficking of CX43 from the early endosome to the late endosome in the absence of WWP1 accompanied by an increase in total CX43 protein, we hypothesized that recycling of CX43 might be affected. To investigate this possibility, endogenous WWP1 was knocked down in HeLa-CX43 cells using a targeting siRNA pool. The effect of WWP1 on CX43 recycling was measured through immunofluorescent staining of PMA treated HeLa-CX43 cells using a recycling endosomal marker (RAB11) and CX43 antibodies. Between thirty to forty cells were selected for Pearson's coefficient of co-localization calculations. Values were averaged and compared relative to the Non-targeting siRNA. Our data shows that loss of function of WWP1 is associated with increased recycling to the plasma membrane compared to NT-siRNA or to untransfected cells (Fig. 4.6), thus corroborating the physiological role of WWP1 in the intracellular of CX43.

## 4.4. DISCUSSION

The cellular pathways that degrade CX43 have been previously characterized and debated, with evidence linking stabilization of CX43 to inhibition of either the proteasome or the lysosome (Dunn et al., 2012; Falk et al., 2014). Further, a role for NEDD4-mediated ubiquitylation in promoting the degradation of CX43 though the autophagy pathway (which is also dependent on lysososmal activity) has also been described (Falk et al., 2012). Currently, it is believed that the role of proteasomal inhibition on CX43 stabilization is an indirect effect of proteasomal degradation of other substrates (Dunn et al., 2012). This may be due, in part, to the fact that proteasomal inhibition leads to the accumulation of polyubiquitylated proteins, resulting in the depletion of the cellular ubiquitin pool required for the remainder of the cellular degradative pathways. Alternatively, it has been postulated that proteasomal inhibition may regulate the stability of CX43 interacting proteins that play a critical role in CX43 life cycle. In particular, it has been shown that a mutant form of CX43 which cannot be ubiquitylated (as all lysine residues were mutated to arginine) responded to proteasomal inhibition similarly to wild type CX43 (Dunn et al., 2012). It was determined that the mechanism for the observed stabilization of CX43 at the plasma membrane upon proteasomal inhibition resulted from the stabilization of AKT upon proteasomal inhibition, as AKT is regulated by the ubiquitin-proteasome pathway (Dunn et al., 2012). In turn, AKT was shown to directly phosphorylate CX43, and this post-translational modification inhibited the internalization of CX43, thereby enhancing CX43 stability at the plasma membrane. In this study we demonstrated that the ubiquitin ligase activity of

WWP1 was necessary for the lysosomal degradation of CX43, confirming the importance of this pathway in the lifecycle of CX43.

In particular, our data point to the fact that WWP1 acts on CX43 that is already internalized. Certainly the intracellular localization of WWP1 supports this hypothesis. Previous studies have reported that WWP1 localizes to the early endosome (Zhi and Chen, 2012). Similarly, we showed co-localization of mCherry-WWP1 with the early endosomal marker EEA1. Further, PMA-treated HeLa-CX43 cells transfected with either catalytically active or inactive forms of WWP1 showed no statistically significant difference in the co-localization of CX43 with EEA1, nor were these values significantly different from untransfected cells that were PMA-stimulated. Collectively, this suggests that endocytosis of CX43 is independent of the ligase activity of WWP1. It was only after this step in the process that the ubiquitin ligase activity of WWP1 showed a significant effect in promoting the trafficking of CX43 from the early endosome to the late endosome and on to the lysosome for degradation. Importantly, in all of our assays, the C886S mutant yielded phenotypes that were statistically indistinguishable from untransfected cells, suggesting that this construct has no additional dominant negative effects.

We also show that the ligase-dependent effects of WWP1 are not overexpression artifacts, as knockdown of WWP1 resulted in decreased co-localization of CX43 and CD63 in the late endosome and increased co-localization of CX43 with the recycling marker RAB11. Our finding is in agreement with a previous study that showed the co-localization of CX43 with RAB11 in the presumptive recycling endosome in MDCK cells as they were exiting mitosis (Boassa et al., 2010). In addition, a study using Sertoli

cells (somatic cells of the testis) transfected with CX43-mCherry and RAB11-GFP indicated the co-localization of CX43 with RAB11 one hour after induction of GJ internalization (Gilleron et al., 2011). Therefore, these reports are in agreement with our findings of CX43 recycling to the plasma membrane. Our data suggest that WWP1 may be mechanistically linked to this default recycling pathway. In the future, it will be important to examine how expression of WWP1 may change or may be post-translationally modified during processes like mitosis to allow for changes in the rate of CX43 recycling.

Taken together our data showed that WWP1-mediated ubiquitylation in the early endosome is required for CX43 turnover. However, the internalization of CX43 does not require the ubiquitin ligase activity of WWP1. We hypothesize that that process may be driven by phosphorylation of CX43 as well as its ubiquitylation by NEDD4 and SMURF2. Once internalized, additional ubiquitylation signals from WWP1 direct CX43 to the late endosome and on to the lysosome for degradation. If this signal is not administered (such as occurs during WWP1 knockdown), the CX43 is recycled back to the plasma membrane. This finding suggests the physiological role of WWP1 in the recycling pathway for CX43. The increased recycling of CX43 is associated with increased CX43 levels on the plasma membrane which in turn is associated with increased GJIC. Determining the specificity of the regulation of WWP1, and thus of CX43, will prove valuable in understanding normal cellular homeostasis as well as providing a first step to developing new therapeutics against conditions characterized by dysregulation of WWP1, CX43, or both.

## 4.5. FIGURES

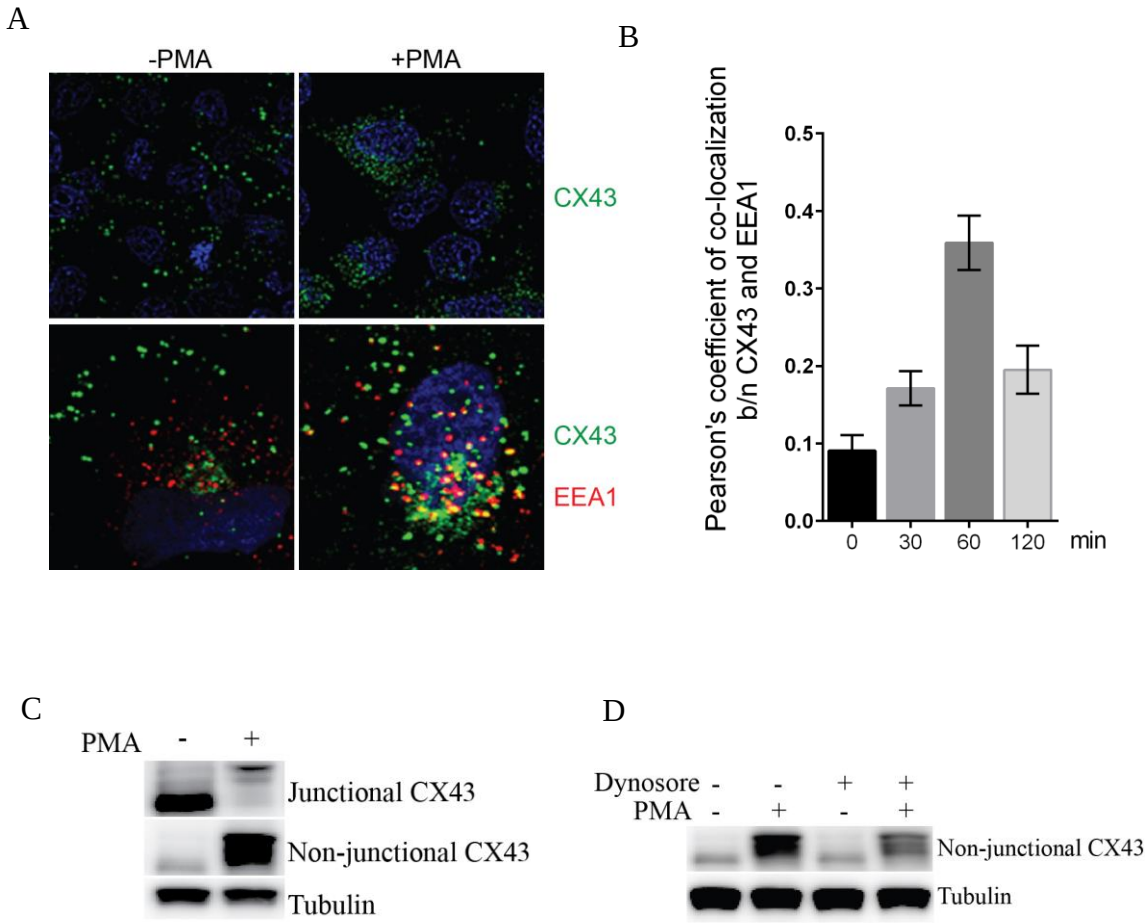


Figure 4.1. Kinetics of PMA-induced internalization of CX43. A. HeLa-CX43 were fluorescently labelled using antibodies directed against CX43 (green) and the endosomal marker EEA1 (red) in the presence and absence of PMA. Treatment of cells with PMA caused endocytosis of CX43. B. HeLa-CX43 cells were treated with PMA for the indicated times and then fluorescently labelled with anti-CX43 and anti-EEA1 antibodies. A bar graph showing the mean and SEM of Pearson's coefficient of co-localization (n=25). Maximal internalization was observed with 1hour of PMA treatment so this was utilized in subsequent experiments. C. 293T cells over expressing CX43 were treated with PMA and the level of plasma membrane and cytoplasmic CX43 was analyzed using the Triton X-100 solubility assay. PMA decreased the level of junctional (plasma membrane) with a concomitant increase in the non-junctional (cytoplasmic) CX43 level. D. Inhibition of the CME pathway in 293T cells using 80 µM of dynosore for 2 hours counteracted the PMA-induced internalization of CX43 (lane 4) suggesting that PMA induced endocytosis is mediated by the Clatherin machinery.

A

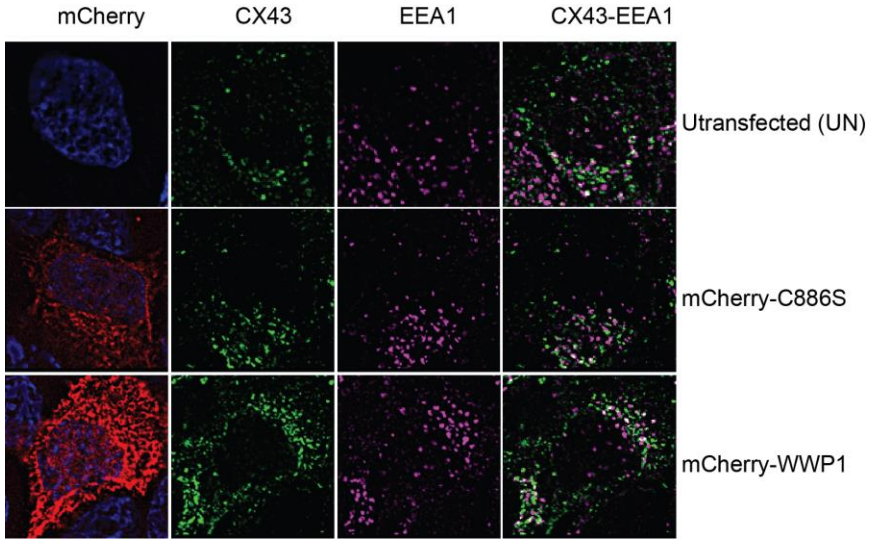


B

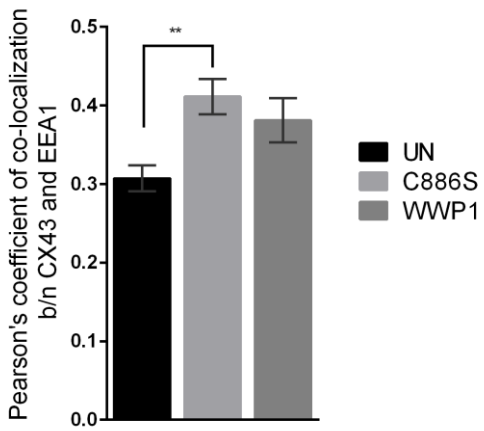


Figure 4.2. WWP1 activity is not required for CX43 internalization. A. PMA-stimulated HeLa-CX43 cells were transfected with either mCherry-WWP1 or mCherry-C886S (red) and compared followed by immunofluorescent staining using anti-CX43 (green) and EEA1 (purple) antibodies. Overlap of the latter two markers appears white. Little difference can be visualized among the three groups. Representative images from at least three independent experiments are shown here. B. Pearson's coefficient of co-localization was calculated using the co-localization threshold plugin of ImageJ software (NIH). A bar graph showing the average of Pearson's coefficient of co-localization for mCherry expressing cells or untransfected (n=25), ±SEM. The analysis revealed the WWP1 ligase activity is not necessary for CX43 co-localization with the early endosome. One-way ANOVA was used to calculate significance.

A

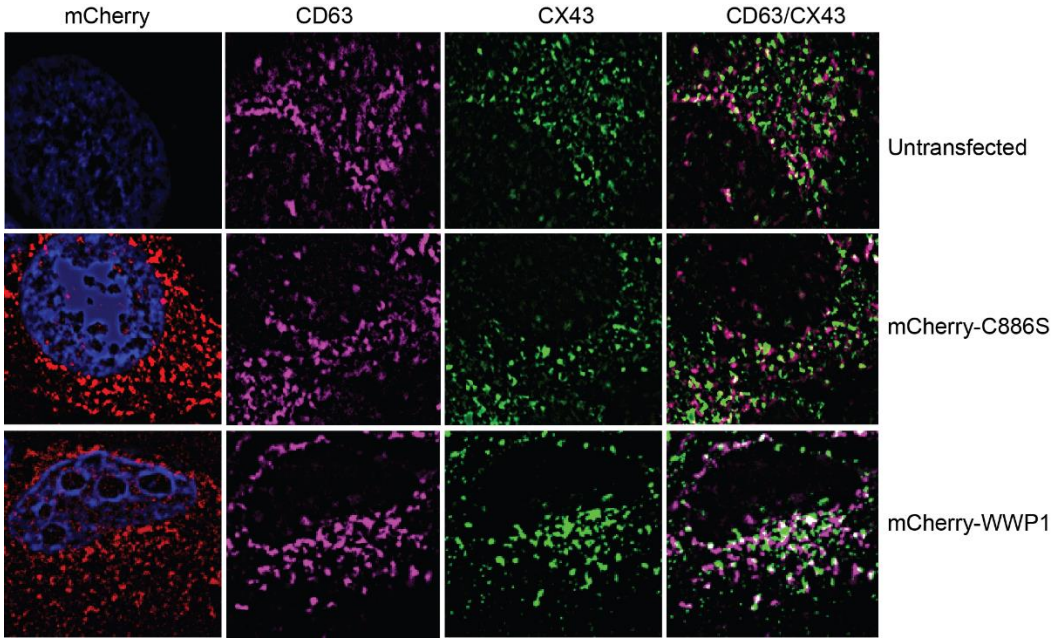
mCherry
CD63
CX43
CD63/CX43
Untransfected
mCherry-C886S
mCherry-WWP1

B

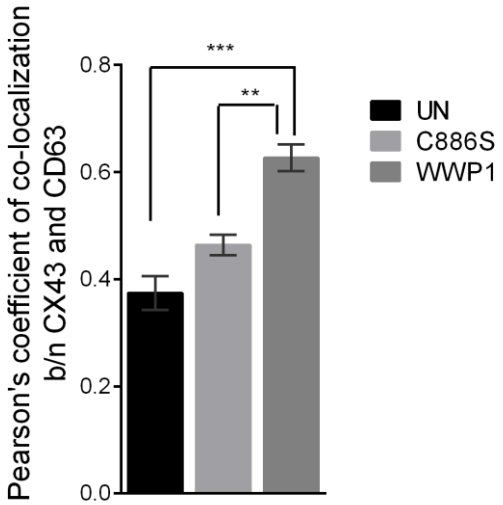
Pearson's coefficient of co-localization b/n CX43 and CD63
0.0
0.2
0.4
0.6
0.8
***
**
UN
C886S
WWP1

Figure 4.3. WWP1 mediates increased trafficking of CX43 form the early endosome to the late endosome. A. PMA-treated HeLa-CX43 cells were transfected with mCherry-Wwp1 or mCherry-C886S (red) and compared to untransfected cells that were PMA-stimulated (UN). All cells were fluorescently labelled using anti-CX43 (green) and anti-CD63 (purple) antibodies. Co-localization of CX43 and CD63 appears white. Representative images from three independent experiments are shown. B. Bar graph showing the average Pearson's coefficient of co-localization from mCherry expressing cells (n=30), ±SEM. One-way ANOVA was used to calculate significance ($p<0.05$). Our data showed increased co-localization of CX43 with the late endosomal marker CD63 upon overexpression of WWP1 compared with transfection using C886S or untransfected (UN) cells.

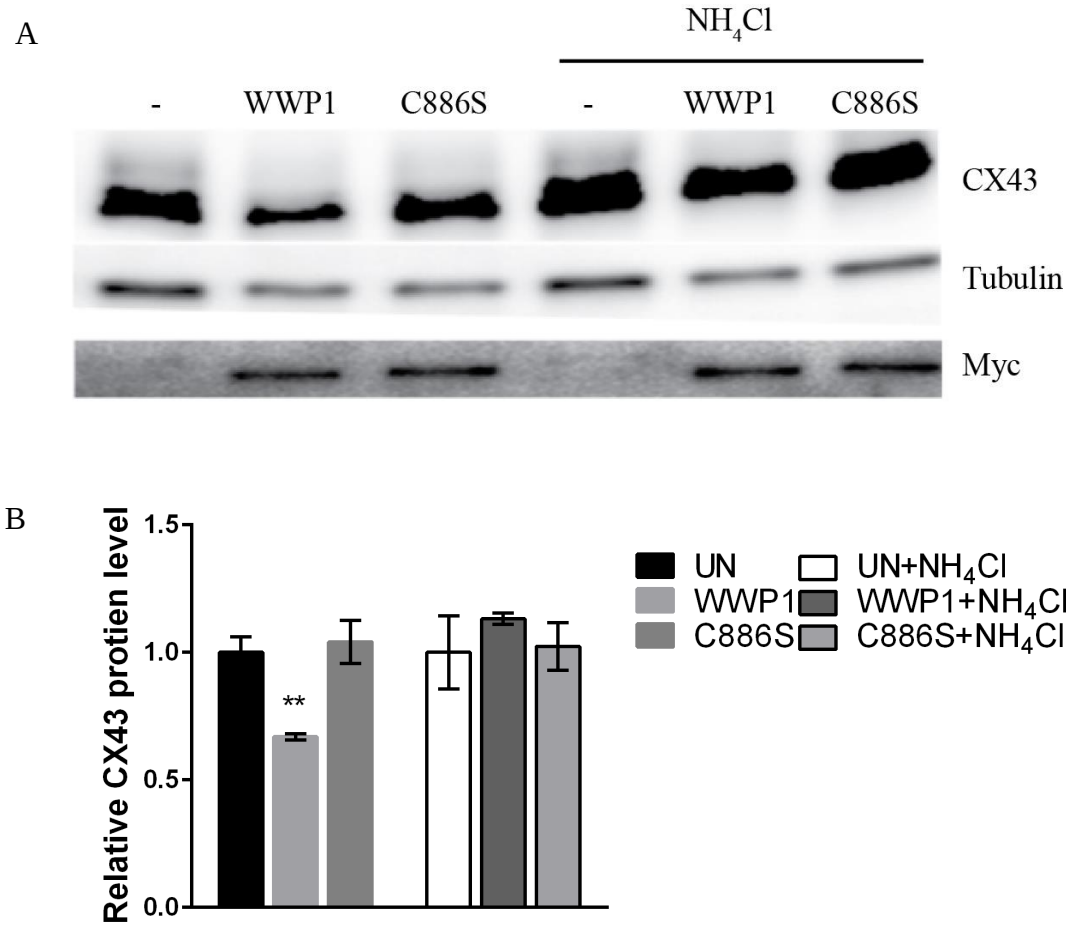


Figure 4.4. WWP1-mediated ubiquitylation leads to lysosomal degradation of CX43. A. HeLa-CX43 cells were transfected either with Myc-WWP1 or Myc-C886S. 48 hours post transfection cells were treated with 100 ng/mL PMA for 1 hour followed by treatment with 25 mM $NH_4Cl$ for 3 hrs. Cells were harvested with Laemmli sample buffer and western blot analysis was performed using anti-CX43, anti-Myc and anti-tubulin antibodies. The Cx43 protein level was decreased upon overexpression of WWP1 however lysosomal inhibition reversed the decrease in Cx43. B. A bar graph showing the average and ± SEM of CX43 level of duplicates relative to untransfected cells. Tubulin was used as a loading control. One-way ANOVA was used to test for significance. While overexpression of WWP1 resulted in a significant a 40% decrease in the amount of CX43, in the presence of lysosomal inhibitors, there was no statistically significant difference among untransfected cells, cells transfected with the ligase-dead version of WWP1, or cells transfected with wild type WWP1. This is consistent with the assertion that WWP1-mediated ubiquitylation promotes lysosomal degradation of CX43.

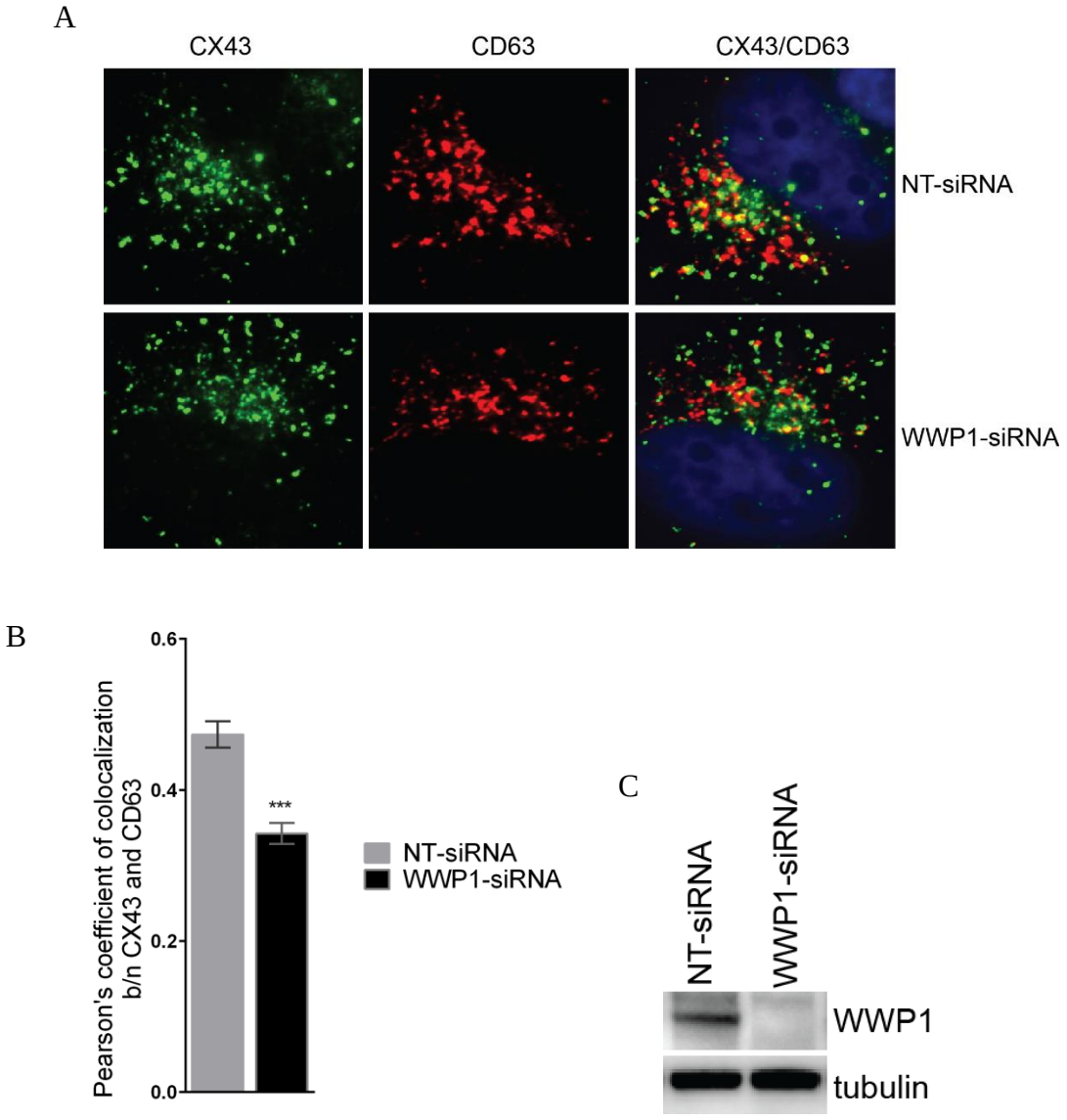


Figure 4.5 Loss of endogenous WWP1 decreases CX43 trafficking to the late endosomes. A. HeLa-CX43 cells were transfected with WWP1 targeting siRNA or non-targeting siRNA (NT-siRNA) followed by immunofluorescent stating using anti-CX43 (green) and anti-CD63 (red) antibodies, with overlap in yellow. B. A bar graph showing the average Pearson's coefficient of co-localization showed decreased co-localization of CX43 with CD63 upon siRNA-mediated WWP1 knockdown. A Student's t-test was performed to test for significance (n=25), ± SEM ($p<0.001$) C. Western blot showing knockdown of WWP1 in HeLa-CX43 cells.

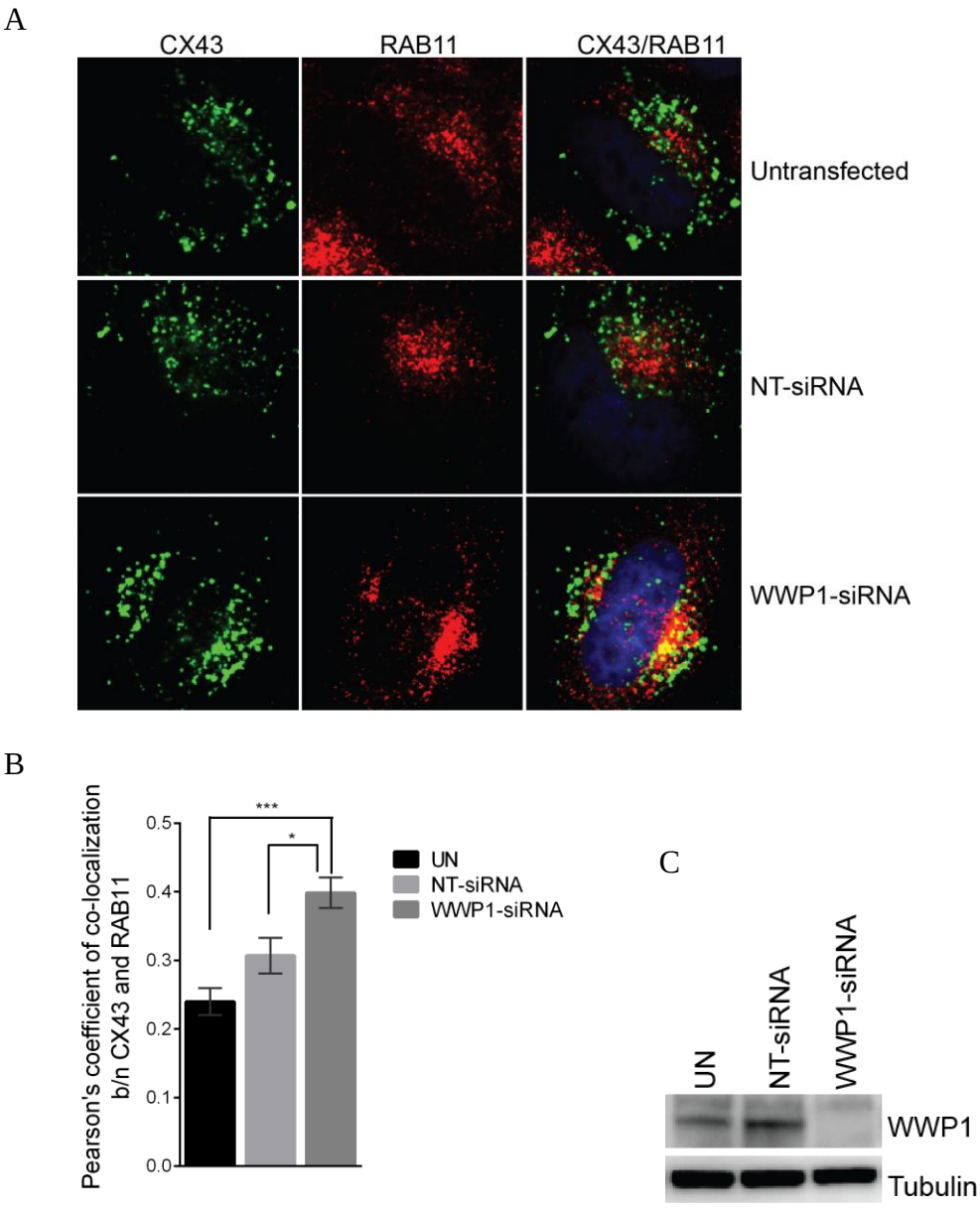


Figure 4.6 Loss of function of WWP1 leads to enhanced CX43 recycling. A. HeLa-CX43 cells were transfected with targeting siRNA pool (WWP1-siRNA) or non-targeting siRNA (NT-siRNA) followed by immunofluorescent labelling using anti-CX43 (green) and anti-RAB11 (red) antibodies with overlap in yellow. Representative images taken from one of three independent experiments are shown. B. A bar graph showing the average Pearson's coefficient of co-localization ±SEM, (n=25).There was a statistically significant ($p<0.00$) increase in the co-localization of CX43 with recycling endosomes upon WWP1-siRNA knockdown. One-way ANOVA was performed to test statistical significance. C. Western blot demonstrating effective knockdown in the cells examined.

# CHAPTER FIVE

## CONCLUDING REMARKS

Post-translational modification through ubiquitylation plays a critical role in a myriad of cellular processes such as signaling, cell proliferation, transcription, translation, DNA repair and cellular homeostasis (Chen and Matesic, 2007; Zhi and Chen, 2012). Ubiquitylation of a given substrate can result in one of a number of outcomes, including proteasomal degradation, a change in subcellular localization, endocytosis from the plasma membrane, signaling, activation or inactivation of enzymatic functions, among others (Weissman, 2001). The temporal and spatial specificity of the ubiquitylation cascade is accomplished via selective substrate binding by E3 ubiquitin ligases (Heride et al., 2014; Hicke and Dunn, 2003). The physiological function of one such E3 ligase, WWP1, has been implicated in a spectrum of cellular process ranging from intracellular protein trafficking and degradation, to cell signaling in apoptosis, bone differentiation and viral budding (Zhi and Chen, 2012). Because of its constellation of functions, it is not surprising that dysfunction of WWP1 has been associated with a number of pathologies including prostate and breast carcinogenesis, neuropathology, osteoporosis and viral infections (Chen et al., 2008; Li et al., 2009; Salah et al., 2012; Shu et al., 2013; Zhi and Chen, 2012). Indeed, our previous work with a mouse model of global WWP1 overexpression demonstrated that WWP1 dysfunction also plays a role in arrhythmogenesis via its regulation of a novel target, the GJ protein CX43. In this study we elucidated the molecular mechanism underlying the regulation of CX43 by WWP1.

In particular, we demonstrated that WWP1 co-immunoprecipitates with CX43 through the carboxy-terminal PPXY motif of CX43. WWP1 has four tandem WW domains that are known to have affinity for PPXY motifs in substrates (Chen et al.,

2008). Consequently, a co-immunoprecipitation assay using a mutant CX43 with a proline to leucine substitution abrogated WWP1 pull down with CX43. These data suggest that WWP1 may directly interact with CX43 through the PY motif although *in vitro* pull down assays using purified GST-tagged WWP1 and CX43 needs to be conducted to show direct interaction. We have also noted that the co-immunoprecipitation was enhanced in the presence of PMA, which is documented to induce MAPK kinase signaling dependent phosphorylation of CX43 (Solan and Lampe, 2005, 2014). Based on this, we speculate that WWP1 has a higher affinity for phosphorylated CX43, although this needs to be confirmed through co-immunoprecipitation experiments using antibodies against phosphorylated and non-phosphorylated forms of CX43 as well as co-IP using mutant CX43 that is resistant to phosphorylation or a phosphomimicking mutant CX43. Alternatively, the increased co-immunoprecipitation of WWP1 and CX43 may be the consequence of greater quantities of these proteins localizing to the same intracellular compartment. This could arise 1) if WWP1 were a resident early endosome-associated protein and PMA increased the delivery of CX43 to the early endosome, 2) if PMA affected the intracellular distribution of WWP1 and caused recruitment of WWP1 to the early endosome, possibly by phosphorylation, or 3) some combination of the two. These possibilities remain to be sorted out by performing experiments that identify the subcellular localization of WWP1 in the presence and absence of PMA. The possibility that WWP1 is regulated by phosphorylation is not new, in fact some members of the NEDD4 subfamily of E3 ligases have been reported to be regulated through phosphorylation. For instance, protein kinase

A (PKA) and serum/glucocorticoid kinase 1(SGK1) dependent phosphorylation of NEDD4-2 inhibited its ligase activity (Ismail et al., 2014).

The association of WWP1 and CX43 was important in the ubiquitylation of CX43. Specifically, we found that WWP1 targets CX43 for K27- and K29-linked polyubiquitylation, and this modification leads to increased CX43 turnover and subsequent decrease in GJIC. Our data indicate that K27- and K29-linked ubiquitylation of CX43 is dependent on the ligase activity of WWP1. Even though the mutant WWP1 C886S, which we demonstrate does not appear to exert a dominant negative effect in this system, is able to bind CX43, it was unable to conjugate a polyubiquitin chain and therefore did not result in CX43 turnover and subsequent reduction in GJIC. Although previous studies have implicated multi-mono-ubiquitylation of CX43 as being important in inducing its internalization (Girao et al., 2009), our data highlight a different linkage, K27- and K29- polyubiquitylation of CX43 that is associated with CX43 turnover. K29-linked polyubiquitin linkage is rare and has been described to be conjugated by the HECT E3 ligase ITCH on its substrate DELTEX causing its trafficking to the lysosome (Chastagner et al., 2006). The fact that CX43 is regulated by several E3 ligases is intriguing, although not unique since regulation by multiple E3 ligases is well documented for other substrates including EGFR (Eden et al., 2012) and p53 (Hock and Vousden, 2014). However, it would be worth identifying the types of ubiquitylation mediated by these E3 ligases since it is known that various ubiquitin linkages have unique conformations and are differentially recognized by UIMs of adaptor proteins (Trempe, 2011).

To determine the cellular mechanism by which CX43 was turned over upon ubiquitylation by WWP1, we examined how intracellular trafficking of CX43 was affected by changes in WWP1 activity. We found that WWP1-mediated ubiquitylation of CX43 led to increased trafficking of CX43 from the early endosome to the late endosome when compared to cells transfected with the dead ligase mutant C886S and to untransfected, PMA-stimulated cells. However, the co-localization of CX43 with early endosome marker EEA1 after PMA treatment did not significantly differ among untransfected HeLa-Cx43 cells, cells overexpressing WWP1, or cells overexpressing C886S, suggesting that WWP1 might not be involved in CX43 endocytosis. On the other hand, PMA is known to induce CX43 phosphorylation and internalization (Leithe and Rivedal, 2004d; Rivedal and Leithe, 2005; Sirnes et al., 2009; Sirnes et al., 2008) and since the cells have been treated with PMA in nearly all of our experiments, we suggest that CX43 phosphorylation is driving internalization, possibly by recruiting other E3 ligases. It is noteworthy that previous studies have associated ubiquitylation of CX43 by two other E3 ligases, NEDD4 and SMURF2, with increased CX43 internalization with no net change in total CX43 level (Fykerud et al., 2012; Girao et al., 2009). Application of a lysosomal inhibitor abrogated WWP1-mediated degradation of CX43 regardless of the ligase activity of WWP1 further corroborating our previous data that showed increased CX43 trafficking to the late endosomes due to WWP1 ligase activity.

Consistent with these changes reflecting a physiological role for WWP1 rather than being an overexpression artifact, knockdown experiments revealed that loss of endogenous WWP1 resulted in increased CX43 on the plasma membrane. Further, we also noted increased co-localization of CX43 and the recycling endosome marker RAB11

in the absence of WWP1, suggesting that an endogenous recycling pathway for CX43 exists. Certainly, precedent for this assertion was established in a previous study that showed the co-localization of mCherry-tagged CX43 with GFP-tagged RAB11 in Sertoli cells (Gilleron et al., 2011). Further, overexpression of WWP1 resulted in decreased co-localization of CX43 with the recycling endosomes compared to the overexpression of the dead ligase WWP1, supporting the hypothesis that the activity of WWP1 is a lynchpin in this bifurcation of the CX43 intracellular trafficking pathway.

Based on these observations we put forth the working model illustrated in Fig. 5.1. NEDD4- and SMURF2-mediated ubiquitylation of CX43 along with PMA-induced phosphorylation promotes the internalization of CX43 from the plasma membrane via an association of ubiquitylated CX43 with the CME machinery. Once the annular junction is disassembled and reaches the early endosome, it interacts with WWP1 which may be resident to that subcellular compartment or recruited there by PMA. K27- and K29-polyubiquitylation of CX43 by WWP1 promote the trafficking of CX43 from the early endosome to the late endosome and subsequently on to the lysosome for degradation. In the absence of WWP1, a default recycling pathway is activated, routing some or all of the CX43 back to the plasma membrane where it can be reincorporated into GJ plaques.

GJs play important roles in critical cellular processes including growth and differentiation, signaling, and homeostasis. Dysregulation of GJ s has been implicated in a number of pathologies including arrhythmia, skin disorders, cataracts, neuropathogenesis, and carcinogenesis (Gerido and White, 2004; Krutovskikh and Yamasaki, 1997; Laird, 2006; Severs et al., 2004). Here we described the molecular mechanisms underlying the regulation of a novel target of WWP1, the GJ protein CX43.

Drug discovery research targeting posttranslational modifications have made great advances in finding therapeutic drugs. Drugs targeting CX43 phosphorylation have being developed and are on trial to treat heart diseases (Kim and Fishman, 2013; Tribulova et al., 2008). Therapeutic approaches targeting the ubiquitylation cascade are also emerging. For instance, cancer therapeutic drugs that inhibit the proteasome are on the market and in clinical trial for lymphoma (Landre et al., 2014). However, this approach is not specific and has numerous side effects. In this regard, E3 ligases are potentially better drug targets for consideration since they determine substrate specificity in the ubiquitylation process. In particular, strategies focusing on finding small molecules that disrupt the interaction of E3 ligases with their substrates will help in designing better and more specific therapeutic drugs. One example for such an approach is the drug, Nutlin, a small molecule disrupting the interaction of the E3 ligase MDM2 and p53. MDM2 is up regulated in cancer and targets p53 for ubiquitylation causing its degradation.

Similarly, WWP1 over expression is associated with arrhythmogenesis in the transgenic mouse model our lab has described, while the *Wwp1* knockout is viable and fertile with a normal lifespan (Shu et al., 2013). This suggests that WWP1 may be a good target for small molecule inhibition in the treatment of pathologies associated with acquired loss of CX43, such as is seen in arrhythmogenesis. Based on the data presented here, we would predict that inhibition of WWP1 would allow for more recycling of CX43 to the plasma membrane, increased GJIC, and restored electroconduction of the heart. However, it remains to be determined if the observations described here in HeLa and 293T cells apply directly to the regulation of CX43 in cardiomyocytes. On the other hand, has been suggested to have tumor suppressive role in the initiation of certain types

of cancer contrary to WWP1 which is suggested to have a protooncogenic role in certain cancer types. Therefore, findings from this study represent an important first step in the path towards development of therapeutic drugs targeting the interaction of WWP1 and CX43 that may underlie numerous pathologies.

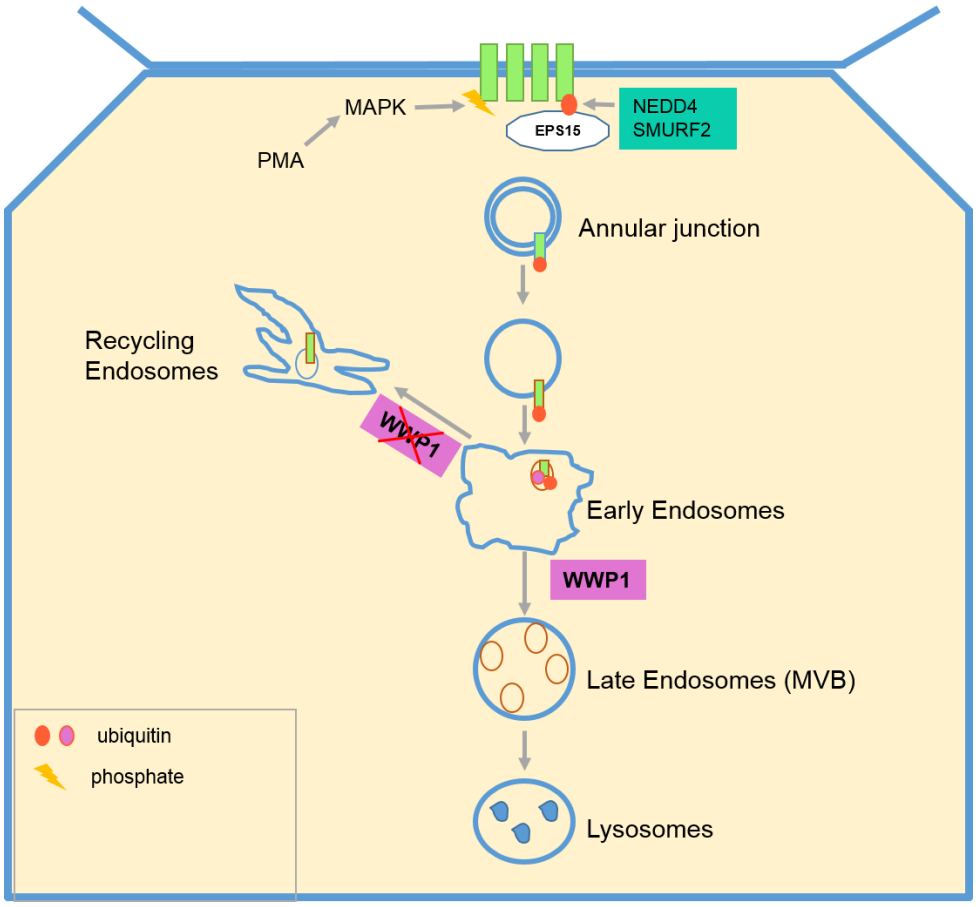


Figure 5.1. A model depicting the life cycle of CX43. CX43 on the plasma membrane is targeted by the E3 ligases NEDD4 and SMURF2 in the presence of PMA causing its endocytosis as a double membrane vesicle termed annular junction. Annular junctions are processed into single membrane bound organelles that eventually fuse with the early endosome. Further ubiquitylation of CX43 by WWP1 in the early endosome leads to increased trafficking of CX43 to the late endosome and from there to the lysosome for degradation. Loss of function of WWP1 leads to CX43 recycling to the plasma membrane.

## REFERENCES


Ahmad, S., Diez, J.A., George, C.H., and Evans, W.H. (1999). Synthesis and assembly of connexins in vitro into homomeric and heteromeric functional gap junction hemichannels. Biochem J *339 ( Pt 2)*, 247-253.

Andersen, K.M., Hofmann, K., and Hartmann-Petersen, R. (2005). Ubiquitin-binding proteins: similar, but different. Essays Biochem *41*, 49-67.

Beardslee, M.A., Laing, J.G., Beyer, E.C., and Saffitz, J.E. (1998). Rapid turnover of connexin43 in the adult rat heart. Circulation Research *83*, 629-635.

Bernassola, F., Karin, M., Ciechanover, A., and Melino, G. (2008). The HECT family of E3 ubiquitin ligases: multiple players in cancer development. Cancer Cell *14*, 10-21.

Boassa, D., Solan, J.L., Papas, A., Thornton, P., Lampe, P.D., and Sosinsky, G.E. (2010). Trafficking and recycling of the connexin43 gap junction protein during mitosis. Traffic *11*, 1471-1486.

Bonifacino, J.S., and Weissman, A.M. (1998). Ubiquitin and the control of protein fate in the secretory and endocytic pathways. Annu Rev Cell Dev Biol *14*, 19-57.

Bremm, A., Freund, S.M., and Komander, D. (2010). Lys11-linked ubiquitin chains adopt compact conformations and are preferentially hydrolyzed by the deubiquitinase Cezanne. Nat Struct Mol Biol *17*, 939-947.

Cao, Y., and Zhang, L. (2013). A Smurf1 tale: function and regulation of an ubiquitin ligase in multiple cellular networks. Cell Mol Life Sci *70*, 2305-2317.

Carrano, A.C., Dillin, A., and Hunter, T. (2014). A Kruppel-like factor downstream of the E3 ligase WWP-1 mediates dietary-restriction-induced longevity in Caenorhabditis elegans. Nat Commun *5*, 3772.

Carrano, A.C., Liu, Z., Dillin, A., and Hunter, T. (2009). A conserved ubiquitination pathway determines longevity in response to diet restriction. Nature *460*, 396-399.

Chastagner, P., Israel, A., and Brou, C. (2006). Itch/AIP4 mediates Deltex degradation through the formation of K29-linked polyubiquitin chains. EMBO Rep *7*, 1147-1153.

Chen, C., and Matesic, L.E. (2007). The Nedd4-like family of E3 ubiquitin ligases and cancer. Cancer metastasis reviews *26*, 587-604.

Chen, C., Zhou, Z., Liu, R., Li, Y., Azmi, P.B., and Seth, A.K. (2008). The WW domain containing E3 ubiquitin protein ligase 1 upregulates ErbB2 and EGFR through RING finger protein 11. Oncogene *27*, 6845-6855.

Chen, V.C., Kristensen, A.R., Foster, L.J., and Naus, C.C. (2012). Association of connexin43 with E3 ubiquitin ligase TRIM21 reveals a mechanism for gap junction phosphodegron control. J Proteome Res *11*, 6134-6146.

Clague, M.J., and Urbe, S. (2010). Ubiquitin: same molecule, different degradation pathways. Cell *143*, 682-685.

Colussi, C., Rosati, J., Straino, S., Spallotta, F., Berni, R., Stilli, D., Rossi, S., Musso, E., Macchi, E., Mai, A., *et al.* (2011). Nepsilon-lysine acetylation determines dissociation from GAP junctions and lateralization of connexin 43 in normal and dystrophic heart. Proc Natl Acad Sci U S A *108*, 2795-2800.

Cooper, C.D., and Lampe, P.D. (2002). Casein kinase 1 regulates connexin-43 gap junction assembly. J Biol Chem *277*, 44962-44968.

David, D., Nair, S.A., and Pillai, M.R. (2013). Smurf E3 ubiquitin ligases at the cross roads of oncogenesis and tumor suppression. Biochim Biophys Acta *1835*, 119-128.

Debeer, P., Van Esch, H., Huysmans, C., Pijkels, E., De Smet, L., Van de Ven, W., Devriendt, K., and Fryns, J.P. (2005). Novel GJA1 mutations in patients with oculo-dento-digital dysplasia (ODDD). Eur J Med Genet *48*, 377-387.

Desplantez, T., Dupont, E., Severs, N.J., and Weingart, R. (2007). Gap junction channels and cardiac impulse propagation. J Membr Biol *218*, 13-28.

Di Fiore, P.P., Polo, S., and Hofmann, K. (2003). When ubiquitin meets ubiquitin receptors: a signalling connection. Nat Rev Mol Cell Biol *4*, 491-497.

Dunn, C.A., Su, V., Lau, A.F., and Lampe, P.D. (2012). Activation of Akt, not connexin 43 protein ubiquitination, regulates gap junction stability. J Biol Chem *287*, 2600-2607.

Eaton, D.C., Malik, B., Bao, H.F., Yu, L., and Jain, L. (2010). Regulation of epithelial sodium channel trafficking by ubiquitination. Proc Am Thorac Soc *7*, 54-64.

Eden, E.R., Huang, F., Sorkin, A., and Futter, C.E. (2012). The role of EGF receptor ubiquitination in regulating its intracellular traffic. Traffic *13*, 329-337.

Falk, M.M., Fong, J.T., Kells, R.M., O'Laughlin, M.C., Kowal, T.J., and Thevenin, A.F. (2012). Degradation of endocytosed gap junctions by autophagosomal and endo-/lysosomal pathways: a perspective. J Membr Biol *245*, 465-476.

Falk, M.M., Kells, R.M., and Berthoud, V.M. (2014). Degradation of connexins and gap junctions. FEBS Lett *588*, 1221-1229.

Falk, M.M., and Lauf, U. (2001). High resolution, fluorescence deconvolution microscopy and tagging with the autofluorescent tracers CFP, GFP, and YFP to study the structural composition of gap junctions in living cells. Microsc Res Tech *52*, 251-262.

Fang, S., and Weissman, A.M. (2004). A field guide to ubiquitylation. Cell Mol Life Sci *61*, 1546-1561.

Fong, J.T., Kells, R.M., Gumpert, A.M., Marzillier, J.Y., Davidson, M.W., and Falk, M.M. (2012). Internalized gap junctions are degraded by autophagy. Autophagy *8*, 794-811.

Fykerud, T.A., Kjenseth, A., Schink, K.O., Sirnes, S., Bruun, J., Omori, Y., Brech, A., Rivedal, E., and Leithe, E. (2012). Smad ubiquitination regulatory factor-2 controls gap junction intercellular communication by modulating endocytosis and degradation of connexin43. J Cell Sci *125*, 3966-3976.

Gaietta, G., Deerinck, T.J., Adams, S.R., Bouwer, J., Tour, O., Laird, D.W., Sosinsky, G.E., Tsien, R.Y., and Ellisman, M.H. (2002). Multicolor and electron microscopic imaging of connexin trafficking. Science *296*, 503-507.

Gerido, D.A., and White, T.W. (2004). Connexin disorders of the ear, skin, and lens. Biochim Biophys Acta *1662*, 159-170.

Gilleron, J., Carette, D., Fiorini, C., Dompierre, J., Macia, E., Denizot, J.P., Segretain, D., and Pointis, G. (2011). The large GTPase dynamin2: a new player in connexin 43 gap junction endocytosis, recycling and degradation. Int J Biochem Cell Biol *43*, 1208-1217.

Girao, H., Catarino, S., and Pereira, P. (2009). Eps15 interacts with ubiquitinated CA3 and mediates its internalization. Experimental Cell Research *315*, 3587-3597.

Gittens, J.E., and Kidder, G.M. (2005). Differential contributions of connexin37 and connexin43 to oogenesis revealed in chimeric reaggregated mouse ovaries. J Cell Sci *118*, 5071-5078.

Goliger, J.A., and Paul, D.L. (1995). Wounding alters epidermal connexin expression and gap junction-mediated intercellular communication. Mol Biol Cell *6*, 1491-1501.

Goodenough, D.A., and Paul, D.L. (2009). Gap junctions. Cold Spring Harb Perspect Biol *1*, a002576.

Gumpert, A.M., Varco, J.S., Baker, S.M., Piehl, M., and Falk, M.M. (2008). Double-membrane gap junction internalization requires the clathrin-mediated endocytic machinery. FEBS Lett *582*, 2887-2892.

Henne, W.M., Buchkovich, N.J., and Emr, S.D. (2011). The ESCRT pathway. Dev Cell *21*, 77-91.

Heride, C., Urbe, S., and Clague, M.J. (2014). Ubiquitin code assembly and disassembly. Curr Biol *24*, R215-220.

Hertzberg, E.L., Chan, T.C., Roy, C., and Nagy, J.I. (1996). Ubiquitination of the gap junction protein connexin43 (Cx43) may involve protein never assembled into gap junctions. Molecular Biology of the Cell *7*, 538-538.

Hicke, L., and Dunn, R. (2003). Regulation of membrane protein transport by ubiquitin and ubiquitin-binding proteins. Annu Rev Cell Dev Biol *19*, 141-172.

Hock, A.K., and Vousden, K.H. (2014). The role of ubiquitin modification in the regulation of p53. Biochim Biophys Acta *1843*, 137-149.

Huang, F., Kirkpatrick, D., Jiang, X., Gygi, S., and Sorkin, A. (2006). Differential regulation of EGF receptor internalization and degradation by multiubiquitination within the kinase domain. Molecular cell *21*, 737-748.

Hurley, J.H., Lee, S., and Prag, G. (2006). Ubiquitin-binding domains. Biochem J *399*, 361-372.

Ingham, R.J., Gish, G., and Pawson, T. (2004). The Nedd4 family of E3 ubiquitin ligases: functional diversity within a common modular architecture. Oncogene *23*, 1972-1984.

Ismail, N.A., Baines, D.L., and Wilson, S.M. (2014). The phosphorylation of endogenous Nedd4-2 In Na(+)-absorbing human airway epithelial cells. Eur J Pharmacol *732*, 32-42.

Jordan, K., Chodock, R., Hand, A.R., and Laird, D.W. (2001). The origin of annular junctions: a mechanism of gap junction internalization. J Cell Sci *114*, 763-773.

Kamynina, E., and Staub, O. (2002). Concerted action of ENaC, Nedd4-2, and Sgk1 in transepithelial Na(+) transport. Am J Physiol Renal Physiol *283*, F377-387.

Kee, Y., and Huibregtse, J.M. (2007). Regulation of catalytic activities of HECT ubiquitin ligases. Biochem Biophys Res Commun *354*, 329-333.

Kim, E., and Fishman, G.I. (2013). Designer gap junctions that prevent cardiac arrhythmias. Trends Cardiovasc Med *23*, 33-38.

Kirchhausen, T., Owen, D., and Harrison, S.C. (2014). Molecular structure, function, and dynamics of clathrin-mediated membrane traffic. Cold Spring Harb Perspect Biol *6*, a016725.

Kjenseth, A., Fykerud, T.A., Sirnes, S., Bruun, J., Yohannes, Z., Kolberg, M., Omori, Y., Rivedal, E., and Leithe, E. (2012). The gap junction channel protein connexin 43 is covalently modified and regulated by SUMOylation. J Biol Chem *287*, 15851-15861.

Komuro, A., Imamura, T., Saitoh, M., Yoshida, Y., Yamori, T., Miyazono, K., and Miyazawa, K. (2004). Negative regulation of transforming growth factor-beta (TGF-beta) signaling by WW domain-containing protein 1 (WWP1). Oncogene *23*, 6914-6923.

Krutovskikh, V., and Yamasaki, H. (1997). The role of gap junctional intercellular communication (GJIC) disorders in experimental and human carcinogenesis. Histol Histopathol *12*, 761-768.

Krutovskikh, V., and Yamasaki, H. (2000). Connexin gene mutations in human genetic diseases. Mutat Res *462*, 197-207.

Laine, A., and Ronai, Z. (2007). Regulation of p53 localization and transcription by the HECT domain E3 ligase WWP1. Oncogene *26*, 1477-1483.

Laird, D.W. (2005). Connexin phosphorylation as a regulatory event linked to gap junction internalization and degradation. Biochim Biophys Acta *1711*, 172-182.

Laird, D.W. (2006). Life cycle of connexins in health and disease. Biochem J *394*, 527-543.

Laird, D.W., Puranam, K.L., and Revel, J.P. (1991). Turnover and phosphorylation dynamics of connexin43 gap junction protein in cultured cardiac myocytes. Biochem J *273(Pt 1)*, 67-72.

Laird, D.W., and Revel, J.P. (1990). Biochemical and immunochemical analysis of the arrangement of connexin43 in rat heart gap junction membranes. J Cell Sci *97 ( Pt 1)*, 109-117.

Lampe, P.D., and Lau, A.F. (2004). The effects of connexin phosphorylation on gap junctional communication. Int J Biochem Cell Biol *36*, 1171-1186.

Landre, V., Rotblat, B., Melino, S., Bernassola, F., and Melino, G. (2014). Screening for E3-Ubiquitin ligase inhibitors: challenges and opportunities. Oncotarget.

Lauf, U., Giepmans, B.N., Lopez, P., Braconnot, S., Chen, S.C., and Falk, M.M. (2002). Dynamic trafficking and delivery of connexons to the plasma membrane and accretion to gap junctions in living cells. Proc Natl Acad Sci U S A *99*, 10446-10451.

Leithe, E., Kjenseth, A., Sirnes, S., Stenmark, H., Brech, A., and Rivedal, E. (2009). Ubiquitylation of the gap junction protein connexin-43 signals its trafficking from early endosomes to lysosomes in a process mediated by Hrs and Tsg101. J Cell Sci *122*, 3883-3893.

Leithe, E., and Rivedal, E. (2004a). Epidermal growth factor regulates ubiquitination, internalization and proteasome-dependent degradation of connexin43. J Cell Sci *117*, 1211-1220.

Leithe, E., and Rivedal, E. (2004b). Epidermal growth factor regulates ubiquitination, internalization and proteasome-dependent degradation of connexin43. J Cell Sci *117*, 1211-1220.

Leithe, E., and Rivedal, E. (2004c). Ubiquitination and down-regulation of gap junction protein connexin-43 in response to 12-O-tetradecanoylphorbol 13-acetate treatment. J Biol Chem *279*, 50089-50096.

Leithe, E., and Rivedal, E. (2004d). Ubiquitination and down-regulation of gap junction protein connexin-43 in response to 12-O-tetradecanoylphorbol 13-acetate treatment. Journal of Biological Chemistry *279*, 50089-50096.

Leithe, E., and Rivedal, E. (2007). Ubiquitination of gap junction proteins. J Membr Biol *217*, 43-51.

Leithe, E., Sirnes, S., Omori, Y., and Rivedal, E. (2006). Downregulation of gap junctions in cancer cells. Crit Rev Oncog *12*, 225-256.

Leykauf, K., Salek, M., Bomke, J., Frech, M., Lehmann, W.D., Durst, M., and Alonso, A. (2006). Ubiquitin protein ligase Nedd4 binds to connexin43 by a phosphorylation-modulated process. J Cell Sci *119*, 3634-3642.

Li, Y., Zhou, Z., Alimandi, M., and Chen, C. (2009). WW domain containing E3 ubiquitin protein ligase 1 targets the full-length ErbB4 for ubiquitin-mediated degradation in breast cancer. Oncogene *28*, 2948-2958.

Lim, K.L., Chew, K.C., Tan, J.M., Wang, C., Chung, K.K., Zhang, Y., Tanaka, Y., Smith, W., Engelender, S., Ross, C.A., *et al.* (2005). Parkin mediates nonclassical, proteasomal-independent ubiquitination of synphilin-1: implications for Lewy body formation. J Neurosci *25*, 2002-2009.

Lim, K.L., Dawson, V.L., and Dawson, T.M. (2006). Parkin-mediated lysine 63-linked polyubiquitination: a link to protein inclusions formation in Parkinson's and other conformational diseases? Neurobiol Aging *27*, 524-529.

Lin, A.E., and Mak, T.W. (2007). The role of E3 ligases in autoimmunity and the regulation of autoreactive T cells. Curr Opin Immunol *19*, 665-673.

Livingston, C.M., Ifrim, M.F., Cowan, A.E., and Weller, S.K. (2009). Virus-Induced Chaperone-Enriched (VICE) domains function as nuclear protein quality control centers during HSV-1 infection. PLoS Pathog *5*, e1000619.

Lorick, K.L., Yang, Y., Jensen, J.P., Iwai, K., and Weissman, A.M. (2006). Studies of the ubiquitin proteasome system. Curr Protoc Cell Biol *Chapter 15*, Unit 15 19.

Luzio, J.P., Parkinson, M.D.J., Gray, S.R., and Bright, N.A. (2009). The delivery of endocytosed cargo to lysosomes. Biochemical Society Transactions *37*, 1019-1021.

Macias, M.J., Wiesner, S., and Sudol, M. (2002). WW and SH3 domains, two different scaffolds to recognize proline-rich ligands. FEBS Lett *513*, 30-37.

McLachlan, E., Manias, J.L., Gong, X.Q., Lounsbury, C.S., Shao, Q., Bernier, S.M., Bai, D., and Laird, D.W. (2005). Functional characterization of oculodentodigital dysplasia-associated Cx43 mutants. Cell Commun Adhes *12*, 279-292.

McLachlan, E., Plante, I., Shao, Q., Tong, D., Kidder, G.M., Bernier, S.M., and Laird, D.W. (2008). ODDD-linked Cx43 mutants reduce endogenous Cx43 expression and function in osteoblasts and inhibit late stage differentiation. J Bone Miner Res *23*, 928-938.

Melino, G., Gallagher, E., Aqeilan, R.I., Knight, R., Peschiaroli, A., Rossi, M., Scialpi, F., Malatesta, M., Zocchi, L., Browne, G., *et al.* (2008). Itch: a HECT-type E3 ligase regulating immunity, skin and cancer. Cell Death Differ *15*, 1103-1112.

Metzger, M.B., Hristova, V.A., and Weissman, A.M. (2012). HECT and RING finger families of E3 ubiquitin ligases at a glance. J Cell Sci *125*, 531-537.

Miyazaki, K., Fujita, T., Ozaki, T., Kato, C., Kurose, Y., Sakamoto, M., Kato, S., Goto, T., Itoyama, Y., Aoki, M., *et al.* (2004). NEDL1, a novel ubiquitin-protein isopeptide ligase for dishevelled-1, targets mutant superoxide dismutase-1. J Biol Chem *279*, 11327-11335.

Miyazaki, K., Ozaki, T., Kato, C., Hanamoto, T., Fujita, T., Irino, S., Watanabe, K., Nakagawa, T., and Nakagawara, A. (2003). A novel HECT-type E3 ubiquitin ligase, NEDL2, stabilizes p73 and enhances its transcriptional activity. Biochem Biophys Res Commun *308*, 106-113.

Moren, A., Imamura, T., Miyazono, K., Heldin, C.H., and Moustakas, A. (2005). Degradation of the tumor suppressor Smad4 by WW and HECT domain ubiquitin ligases. J Biol Chem *280*, 22115-22123.

Musil, L.S., and Goodenough, D.A. (1990). Gap junctional intercellular communication and the regulation of connexin expression and function. Curr Opin Cell Biol *2*, 875-880.

Nielsen, M.S., Nygaard Axelsen, L., Sorgen, P.L., Verma, V., Delmar, M., and Holstein-Rathlou, N.H. (2012). Gap junctions. Compr Physiol *2*, 1981-2035.

Nikko, E., and Andre, B. (2007). Evidence for a direct role of the Doa4 deubiquitinating enzyme in protein sorting into the MVB pathway. Traffic *8*, 566-581.

Ogunjimi, A.A., Briant, D.J., Pece-Barbara, N., Le Roy, C., Di Guglielmo, G.M., Kavsak, P., Rasmussen, R.K., Seet, B.T., Sicheri, F., and Wrana, J.L. (2005). Regulation of Smurf2 ubiquitin ligase activity by anchoring the E2 to the HECT domain. Mol Cell *19*, 297-308.

Piehl, M., Lehmann, C., Gumpert, A., Denizot, J.P., Segretain, D., and Falk, M.M. (2007). Internalization of large double-membrane intercellular vesicles by a clathrin-dependent endocytic process. Molecular Biology of the Cell *18*, 337-347.

Piper, R.C., and Luzio, J.P. (2007). Ubiquitin-dependent sorting of integral membrane proteins for degradation in lysosomes. Current Opinion in Cell Biology *19*, 459-465.

Pizzuti, A., Flex, E., Mingarelli, R., Salpietro, C., Zelante, L., and Dallapiccola, B. (2004). A homozygous GJA1 gene mutation causes a Hallermann-Streiff/ODDD spectrum phenotype. Hum Mutat *23*, 286.

Plant, P.J., Yeger, H., Staub, O., Howard, P., and Rotin, D. (1997). The C2 domain of the ubiquitin protein ligase Nedd4 mediates Ca2+-dependent plasma membrane localization. J Biol Chem *272*, 32329-32336.

Pryor, P.R., and Luzio, J.P. (2009). Delivery of endocytosed membrane proteins to the lysosome. Biochimica Et Biophysica Acta-Molecular Cell Research *1793*, 615-624.

Raiborg, C., and Stenmark, H. (2009). The ESCRT machinery in endosomal sorting of ubiquitylated membrane proteins. Nature *458*, 445-452.

Rivedal, E., and Leithe, E. (2005). Connexin43 synthesis, phosphorylation, and degradation in regulation of transient inhibition of gap junction intercellular communication by the phorbol ester TPA in rat liver epithelial cells. Exp Cell Res *302*, 143-152.

Saffitz, J.E., Hames, K.Y., and Kanno, S. (2007). Remodeling of gap junctions in ischemic and nonischemic forms of heart disease. Journal of Membrane Biology *218*, 65-71.

Salah, Z., Alian, A., and Aqeilan, R.I. (2012). WW domain-containing proteins: retrospectives and the future. Front Biosci (Landmark Ed) *17*, 331-348.

Schneider, C.A., Rasband, W.S., and Eliceiri, K.W. (2012). NIH Image to ImageJ: 25 years of image analysis. Nat Methods *9*, 671-675.

Severs, N.J., Dupont, E., Coppen, S., Halliday, D., Inett, E., Baylis, D., and Rothery, S. (2004). Remodelling of gap junctions and connexin expression in heart disease. Biochimica Et Biophysica Acta-Biomembranes *1662*, 138-148.

Shu, L., Zhang, H., Boyce, B.F., and Xing, L. (2013). Ubiquitin E3 ligase Wwp1 negatively regulates osteoblast function by inhibiting osteoblast differentiation and migration. J Bone Miner Res *28*, 1925-1935.

Sirnes, S., Kjenseth, A., Leithe, E., and Rivedal, E. (2009). Interplay between PKC and the MAP kinase pathway in Connexin43 phosphorylation and inhibition of gap junction intercellular communication. Biochem Biophys Res Commun *382*, 41-45.

Sirnes, S., Leithe, E., and Rivedal, E. (2008). The detergent resistance of Connexin43 is lost upon TPA or EGF treatment and is an early step in gap junction endocytosis. Biochem Biophys Res Commun *373*, 597-601.

Snyder, P.M. (2005). Minireview: regulation of epithelial Na+ channel trafficking. Endocrinology *146*, 5079-5085.

Solan, J.L., and Lampe, P.D. (2005). Connexin phosphorylation as a regulatory event linked to gap junction channel assembly. Biochim Biophys Acta *1711*, 154-163.

Solan, J.L., and Lampe, P.D. (2009). Connexin43 phosphorylation: structural changes and biological effects. Biochem J *419*, 261-272.

Solan, J.L., and Lampe, P.D. (2014). Specific Cx43 phosphorylation events regulate gap junction turnover in vivo. FEBS Lett.

Solan, J.L., Marquez-Rosado, L., Sorgen, P.L., Thornton, P.J., Gafken, P.R., and Lampe, P.D. (2007). Phosphorylation at S365 is a gatekeeper event that changes the structure of Cx43 and prevents down-regulation by PKC. Journal of Cell Biology *179*, 1301-1309.

Staub, O., Dho, S., Henry, P., Correa, J., Ishikawa, T., McGlade, J., and Rotin, D. (1996). WW domains of Nedd4 bind to the proline-rich PY motifs in the epithelial Na+ channel deleted in Liddle's syndrome. Embo j *15*, 2371-2380.

Tanguy, S., Jeyaraman, M., Jiang, Z.S., Fandrich, R.R., and Kardami, E. (2000). Acute remodeling of gap junctions after ischemia and reperfusion produces three distinct groups of cardiomyocytes based on connexin-43 distribution and phosphorylation. Circulation *102*, 135-136.

Thevenin, A.F., Kowal, T.J., Fong, J.T., Kells, R.M., Fisher, C.G., and Falk, M.M. (2013). Proteins and mechanisms regulating gap-junction assembly, internalization, and degradation. Physiology (Bethesda) *28*, 93-116.

Trempe, J.F. (2011). Reading the ubiquitin postal code. Curr Opin Struct Biol *21*, 792-801.

Tribulova, N., Knezl, V., Okruhlicova, L., and Slezak, J. (2008). Myocardial gap junctions: targets for novel approaches in the prevention of life-threatening cardiac arrhythmias. Physiol Res *57 Suppl 2*, S1-s13.

Umebayashi, K., Stenmark, H., and Yoshimori, T. (2008). Ubc4/5 and c-Cbl continue to ubiquitinate EGF receptor after internalization to facilitate polyubiquitination and degradation. Mol Biol Cell *19*, 3454-3462.

van Wijk, S.J., and Timmers, H.T. (2010). The family of ubiquitin-conjugating enzymes (E2s): deciding between life and death of proteins. FASEB journal : official publication of the Federation of American Societies for Experimental Biology *24*, 981-993.

Weissman, A.M. (2001). Themes and variations on ubiquitylation. Nat Rev Mol Cell Biol *2*, 169-178.

Wiesner, S., Ogunjimi, A.A., Wang, H.R., Rotin, D., Sicheri, F., Wrana, J.L., and Forman-Kay, J.D. (2007). Autoinhibition of the HECT-type ubiquitin ligase Smurf2 through its C2 domain. Cell *130*, 651-662.

Wright, M.H., Berlin, I., and Nash, P.D. (2011). Regulation of endocytic sorting by ESCRT-DUB-mediated deubiquitination. Cell Biochem Biophys *60*, 39-46.

Zhi, X., and Chen, C. (2011). WWP1: a versatile ubiquitin E3 ligase in signaling and diseases. Cell Mol Life Sci.

Zhi, X., and Chen, C. (2012). WWP1: a versatile ubiquitin E3 ligase in signaling and diseases. Cellular and molecular life sciences : CMLS *69*, 1425-1434.

Zucchelli, S., Codrich, M., Marcuzzi, F., Pinto, M., Vilotti, S., Biagioli, M., Ferrer, I., and Gustincich, S. (2010). TRAF6 promotes atypical ubiquitination of mutant DJ-1 and alpha-synuclein and is localized to Lewy bodies in sporadic Parkinson's disease brains. Hum Mol Genet *19*, 3759-3770.